Naval Research Laboratory
Monterey, CA 93943-5502

NRL/MR/7543--94-7217

Performance of the Navy's Second Order Closure Version of the NORAPS in Short-Range Refractivity Forecasting During the VOCAR Experiment

GERARD N. VOGEL

Forecast Support Branch

April 1995

Approved for public release; distribution unlimited.

REPORT DOCUMENTATION PAGE

Form Approved
OMB No. 0704-0188

1. AGENCY USE ONLY (*Leave Blank*)	2. REPORT DATE	3. REPORT TYPE AND DATES COVERED
	April 1995	Final

4. TITLE AND SUBTITLE
Performance of the Navy's Second Order Closure Version of the NORAPS in Short-Range Refractivity Forecasting During the VOCAR Experiment

5. FUNDING NUMBERS
PE 0602435N
PN R035S83
AN DN153180

6. AUTHOR(S)
Gerard N. Vogel

7. PERFORMING ORGANIZATION NAME(S) AND ADDRESS(ES)
Naval Research Laboratory
Marine Meteorology Division
Monterey, CA 93943-5502

8. PERFORMING ORGANIZATION REPORT NUMBER
NRL/MR/7543--94-7217

9. SPONSORING/MONITORING AGENCY NAME(S) AND ADDRESS(ES)
Office of Naval Research
Arlington, VA 22217-5660

10. SPONSORING/MONITORING AGENCY REPORT NUMBER

11. SUPPLEMENTARY NOTES

12a. DISTRIBUTION/AVAILABILITY STATEMENT
Approved for public release; distribution unlimited.

12b. DISTRIBUTION CODE

13. ABSTRACT (*Maximum 200 words*)

In conjunction with the Variability of Coastal Atmospheric Refractivity (VOCAR) experiment conducted during late summer 1993 in the Southern California bight region, twice-daily 24 hr forecasts from a second order closure version of the Navy Operational Regional Atmospheric Prediction System (NORAPS) were made. The results from a validation of the model's performance in short-range refractivity forecasting during VOCAR are presented, based on statistical comparisons of model and radiosonde surface and elevated duct occurrence, and trapping layer heights and intensities. Spatial and temporal (diurnal and synoptic) variability of both forecast and observed ducting are discussed. The impact on refractive structure of data assimilation with an incremental update procedure is also examined.

14. SUBJECT TERMS]
VOCAR Refractivity forecasting Coastal refractivity

15. NUMBER OF PAGES
54

16. PRICE CODE

17. SECURITY CLASSIFICATION OF REPORT	18. SECURITY CLASSIFICATION OF THIS PAGE	19. SECURITY CLASSIFICATION OF ABSTRACT	20. LIMITATION OF ABSTRACT
UNCLASSIFIED	UNCLASSIFIED	UNCLASSIFIED	Same as report

NSN 7540-01-280-5500

Standard Form 298 (Rev. 2-89)
Prescribed by ANSI Std 239-18
298-102

TABLE OF CONTENTS

Performance of the Navy's Second Order Closure Version of the NORAPS in Short-Range Refractivity Forecasting During the VOCAR Experiment

1. INTRODUCTION

Accurate forecasts of electromagnetic propagation conditions in coastal regions may now be possible using a sophisticated range-dependent propagation model coupled with atmospheric refractivity data from an advanced high-resolution numerical prediction model. An important objective of the VOCAR (Variability of Coastal Atmospheric Refractivity) experiment is the development and validation of one such coupled mesoscale forecast model / range-dependent propagation model. However, before the difficult process of validation for the coupled system is attempted, a validation alone of the numerical weather prediction model chosen for the VOCAR experiment - the Second Order Closure R&D version of the NORAPS* (SOCM) - is needed. This report presents results from such a validation, providing a detailed statistical examination of the performance of the SOCM in short-range refractivity forecasting during the VOCAR intensive observing period of late summer 1993 in the Southern California bight region.

The verification of SOCM refractivity forecasts is by direct comparisons with mini-radiosondes (MRSs). Specifically, an assessment of SOCM's ability to forecast refractive structure is established, based on statistical comparisons of model and radiosonde duct occurrence, and trapping layer heights and strengths, within the boundary layer. Spatial and temporal variability of both forecast and observed ducting are examined. In order to assess the impact of data assimilation with an incremental update procedure on initial SOCM refractivity forecasts, direct comparisons are made between SOCM background (first guess) and initialized analysis refractivity profiles.

---

* Navy Operational Regional Atmospheric Prediction System

2. SOCM DESCRIPTION

The second order closure version of the NORAPS, with its high vertical and horizontal resolution and sophisticated model physics, is a good choice for coupling with a range-dependent propagation model, since it is capable of realistic and detailed forecasts of refractive structure within the lower atmosphere. SOCM has evolved from the vertically-nested NORAPS model developed at NRL Monterey by Burk and Thompson (1989). Similar to the current operational version of NORAPS, the R&D version is run with a data assimilation cycle which includes a multivariate optimum interpolation (MVOI) analysis (Goerss and Phoebus, 1993) and a nonlinear vertical mode initialization (NLVMI) scheme.

SOCM is a finite difference model formulated in normalized pressure (sigma) coordinates. The model contains prognostic equations for the mean variables - the wind components, liquid water potential temperature and total moisture. Prognostic equations for turbulent kinetic energy, temperature and moisture variances, and their covariances, are given by a second order closure turbulence parameterization. The model's moist thermodynamic calculations include liquid water content and fractional cloudiness; stable precipitation is calculated based upon an assumed cloud droplet distribution function. Cumulus convection is parameterized by a modified Kuo scheme. A detailed radiation scheme computes fluxes of long and short radiation and heating/cooling rates, and provides for explicit cloud/long-wave radiation interaction. Over land, time-dependent budget equations are used to prescribe surface values of temperature and moisture; over the ocean, similarity theory based on bulk parameterization of surface fluxes yields surface temperature and humidity values. For the VOCAR experiment, a sea surface temperature (SST) analysis on a 1 1/4 deg grid, updated daily at 12Z, provided accurate surface forcing for marine surface fluxes.

During VOCAR, SOCM forecasts were initialized at 00Z and 12Z by performing a MVOI analysis, which incorporated quality controlled observations from the operational atmospheric database at the Fleet Numerical Meteorology and Oceanography Center (FNMOC) in Monterey. The OI analysis was performed for 16 constant pressure levels, from 10 mb to 1000 mb. The meteorological variables analyzed were the geopotential height and the wind; the virtual temperature was derived by maintaining an approximate hydrostatic balance between the height and wind fields. During VOCAR, SOCM did not use a moisture analysis; rather, the 12 hr forecast field from the previous model run normally served as the initial moisture field for the

next forecast. In order to reduce interpolation errors and maintain low-level vertical structure throughout the forecast, data assimilation at 12 hr intervals was performed using an incremental update procedure, in which analysis increments (analyzed corrections to first guess fields) were interpolated to model sigma levels rather than constant pressure levels. Before the forecast, a nonlinear vertical mode initialization was used to remove gravity wave noise. Archived global analysis and forecast fields from FNMOC provided time-dependent boundary conditions to SOCM at 12 hr intervals during the forecast.

For the VOCAR experiment, SOCM was run with a 109 x 82 x 30 grid domain, and a 20 km horizontal grid spacing (Figure 1). The model had 14 computational levels within 1 km of the surface, with spacing compacted toward the surface such that 6 levels lay within the first 200 m. Time steps for model dynamics and physics computations were set to 1 min and 6 min, respectively. Model forecasts were limited to 24 hours.

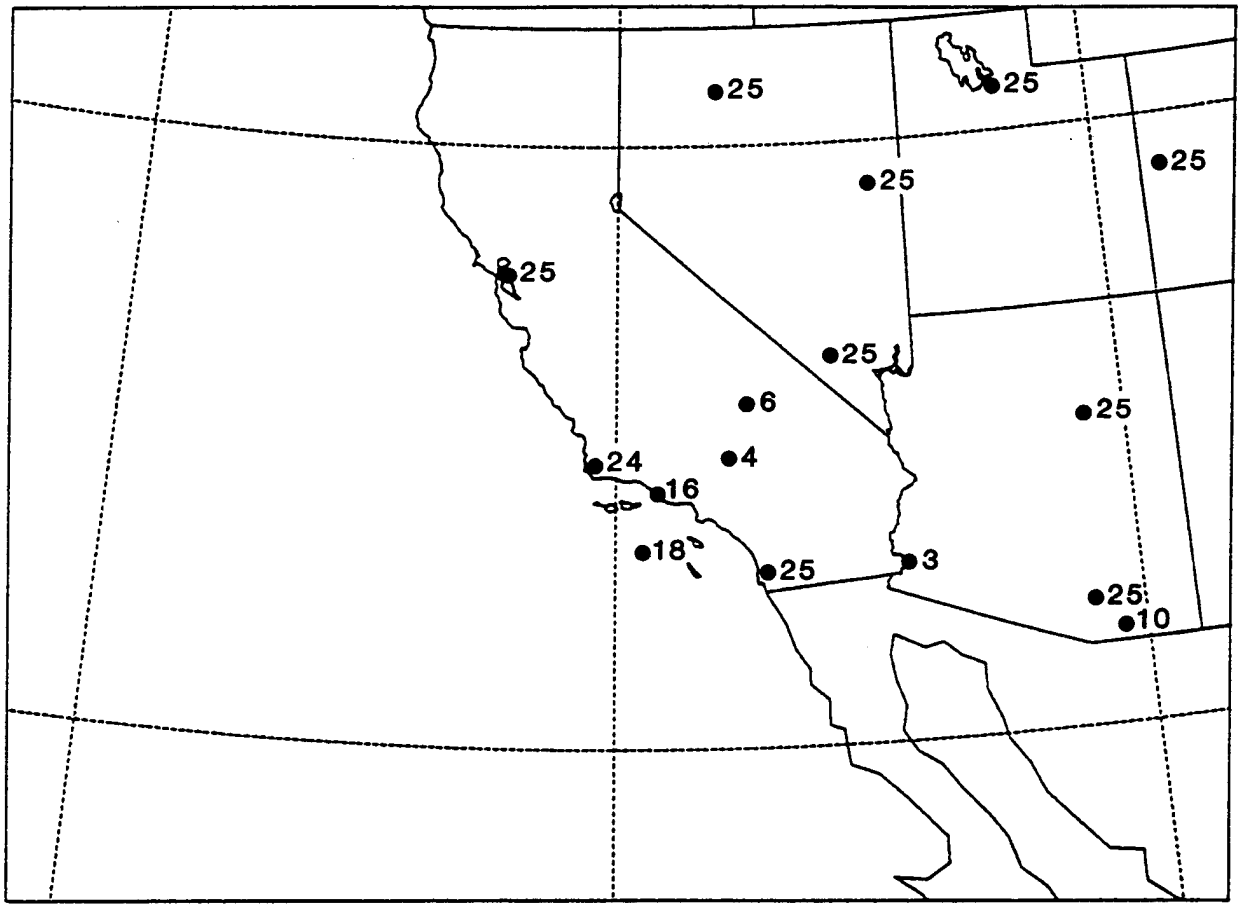

Figure 1. SOCM forecast domain for the VOCAR experiment. Locations and number of conventional (00Z and 12Z) radiosondes available within the FNMOC observational database for model initialization (i.e., analysis) during the forecast period 23 Aug 00Z - 4 Sep 00Z 1993 are shown.

3. DATA

During the VOCAR intensive observing period of August 23 - September 3, 1993, hundreds of miniradiosondes were launched at selected sites within the Southern California bight region. Simultaneously, SOCM forecasts were made every 12 hours for the VOCAR study area. These radiosonde and model data are the two databases utilized in this study. All data comparisons will be limited to the lower troposphere, from the surface to 1.5 km.

3.1 Miniradiosonde

For the VOCAR experiment, miniradiosondes from five coastal sites [North Island (NZY), Camp Pendleton (CPN), Point Vicente (PVN), Point Mugu (NTD) and Vandenberg AFB (VBG)], two island sites [San Clemente (NUC) and San Nicolas (NSI)] and the research vessel Point Sur (PSR) are available for verification of model refractivity forecasts (Figure 2). With the exception of PVN and NUC, all station elevations (i.e., radiosonde launch heights) were within 15 meters of sea level. The VBG site was relocated about four days into the experiment, from a beach location to a slightly higher site several kilometers away. The Point Sur research vessel launched sondes "on-site" (near 33.6 N, 118.9 W) for about a 4 1/2 day period (between 8/26 00Z and 8/30 12Z), as well as 7 other sondes below the latitude of Point Arguello, CA while in transit to and from its "on-site" position.

At all land sites, MRS launches began sometime on the 23rd of August local time; launches were stopped as early as 9/2 1700 PDT at NUC and as late as 9/3 1300 PDT at both VBG and NSI. VOCAR sonde launches were scheduled every four hours from 12Z through 04Z, but not at 08Z (0100 PDT). The Point Sur research vessel released sondes one hour earlier than the other sites, but PSR did include launches at 07Z (midnight PDT). In spite of several missed launches, radiosonde availability throughout the intensive observing period can be rated very good to excellent at all sites with the exception of NTD, which provided only two soundings at 20Z. MRS launches not at scheduled times (including 8 at NSI) and PSR launches outside the area of Figure 2 (i.e., north of 35 N) are excluded from study consideration.

Vaisala miniradiosonde systems were utilized for all VOCAR sonde launches. More advanced Vaisala systems used at NTD, VBG, NUC, NSI and aboard the Point Sur research vessel provided for both up- and down- sonde capability; however, only upsondes are used in this study. A sampling rate of between 2 and 10 seconds (most often 2 sec at sonde

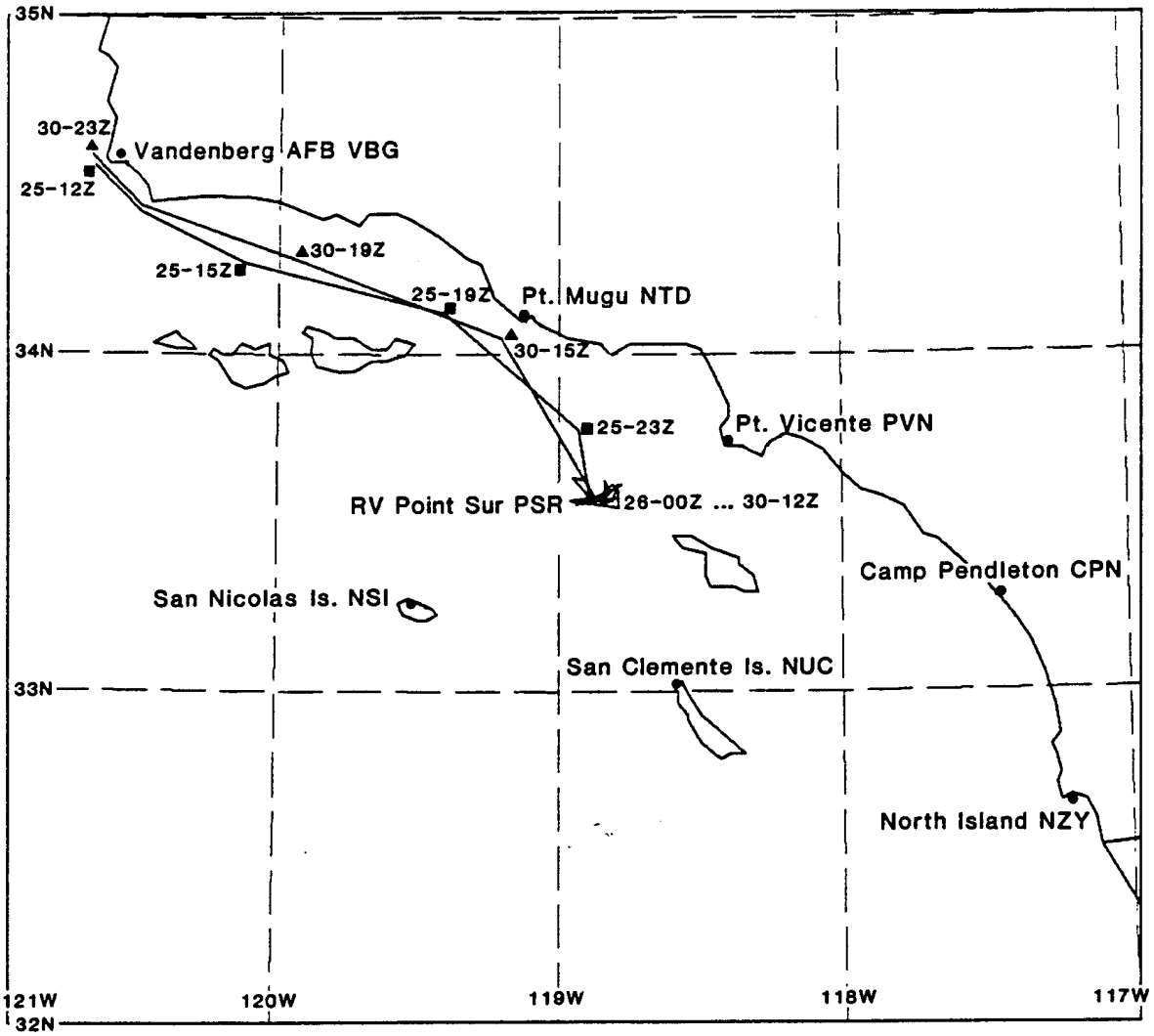

Location	Latitude (N)	Longitude (W)	Elevation (m/msl)
North Island (NZY)	32.73	117.22	6
Camp Pendleton (CPN)	33.28	117.47	10
Point Vicente (PVN)	33.74	118.41	40
Point Mugu (NTD)	34.10	119.12	2
Vandenberg AFB (VBG)			
8/23 16Z - 8/27 16Z	34.56	120.61	1
8/28 00Z - 9/3 20Z	34.60	120.64	15
San Clemente Is. (NUC)	33.02	118.59	60
San Nicolas Is. (NSI)	33.28	119.52	14
Point Sur (PSR)	"On-Site" Avg.		
8/26 00Z - 8/30 12Z	33.59	118.86	9

Figure 2. VOCAR miniradiosonde locations and launch heights. The ship track for the research vessel Point Sur is shown.

initialization) allowed for a very high (i.e., virtually continuous) resolution of atmospheric structure at all sites. A typical VOCAR atmospheric sounding contains a few hundred vertical levels from the surface to 1.5 km.

Prior to use in this study, each VOCAR MRS was carefully scrutinized to assure accuracy and consistency. Where possible, obvious errors were corrected and dubious sounding information deleted. A total of 11 miniradiosondes were considered completely useless and removed from the database; fortunately, two of these had replacement (i.e., relaunch) sondes.

During data processing, modified refractivity values (i.e., M-profiles) were computed from conventional meteorological data (pressure, temperature, humidity and height). Given a MRS refractivity M-profile, all trapping layers from the surface to 1.5 km were found. During this procedure, trapping layers connected by constant M layers were allowed to be combined, forming a deeper trapping layer. It should be pointed out that M-unit and height values (height in meters) defining M-profile data levels are only specified to units (i.e., whole number values); the use of a higher "accuracy" would not only exceed Vaisala instrument capabilities but also would result, for many MRS soundings, in a very large and unwieldy (and thus unacceptable) number of very shallow trapping layers. MRS M-profile trapping layers (base and top heights and corresponding M values) constitute the base data used for comparison with SOCM forecasts of ducting derived from model refractivity profiles.

Time series of MRS trapping layers for individual stations are given in Appendix A. Here, all trapping layers with thicknesses $\geq$ 10 m and M-deficits $\geq$ 2 M-units , from the surface to 1.5 km, are plotted. (Note: the M-deficit is the value of M at the base of the trapping layer minus the value at the top). Of the total 385 miniradiosondes used in this study, only three sondes (8/31 12Z and 9/2 12Z at NTD, and 8/31 00Z at NSI) failed to have at least one trapping layer which met the above plotting specification. In these station plots, the M-deficit of each individual trapping layer is given as one of three distinct categories, which allows the viewer to readily discern the location of dominant trapping layers and their time variations.

3.2 Model

Commencing at 00Z August 23, 1993 and terminating at 00Z September 4, 1993, SOCM 24 hour forecasts for the VOCAR grid domain (Figure 1) were made every 12 hours utilizing the Cray C90 supercomputer at FNMOC. For each forecast run, gridded meteorological data fields were archived at 4 hour forecast intervals. These model data fields were subsequently reformatted and entered into a VOCAR database on a UNIX-based workstation. Although the

translation of SOCM archived forecast data into a GrADS (Grid Analysis and Display System) data format required both horizontal and vertical interpolation of gridded data, the grid resolution of SOCM data in the GrADS format (hereafter, SOCM(GrADS)) is similar to actual model resolution. Specifically, the forecast model runs at a 20 km horizontal resolution with 14 computational levels within 1 km of the terrain surface; the SOCM(GrADS) data grid has a (x,y) spacing of 0.2 deg longitude x 0.1725 deg latitude, with 16 constant height levels from sea level to one kilometer elevation. Given its high data resolution (comparable to the model) and ready availability, SOCM(GrADS) gridded data will be used for this study.

For any selected MRS location, model-derived M-profiles, computed on the SOCM (GrADS) grid, are extracted from the VOCAR database and examined for ducting structure. These model M-profiles correspond to profiles at the nearest SOCM(GrADS) water gridpoint to the MRS site and, where available, to profiles at a SOCM(GrADS) land gridpoint in close proximity to the MRS location. SOCM(GrADS) water and land point locations and terrain heights assigned to each MRS site are shown in Table 1.

Table 1. SOCM(GrADS) water and land gridpoint locations and terrain heights assigned to VOCAR MRS stations.

LOCATION	WATER POINT			LAND POINT		
	LAT (N)	LON (W)	ELV (m/msl)	LAT (N)	LON (W)	ELV (m/msl)
NORTH ISLAND(NZY)	32.77	117.2	0	32.60	117.0	25.3
CAMP PENDLETON(CPN)	33.11	117.4	0	33.29	117.6	1.4
POINT VICENTE(PVN)	33.63	118.4	0	33.80	118.4	1.4
POINT MUGU(NTD)	34.15	119.2	0	34.15	119.0	84.8
VANDENBERG AFB(VBG)						
8/23 16Z - 8/27 16Z	34.49	120.6	0	34.49	120.4	9.6
8/28 00Z - 9/3 20Z	34.67	120.6	0	34.67	120.4	45.8
SAN CLEMENTE IS.(NUC)	32.94	118.6	0	32.94	118.4	0.2
SAN NICOLAS IS.(NSI)	33.29	119.6	0	-----	-----	----
POINT SUR(PSR)	VAR	VAR	0	-----	-----	----
8/26 00Z - 8/30 12Z	33.63	118.8	0	-----	-----	----

Values given here are not actual model gridpoint locations and heights, but rather those from the SOCM(GrADS) grid. As indicated by Table 1, model land point forecasts were not available for either San Nicholas Is. or the research vessel Pt. Sur. The SOCM(GrADS) water gridpoint assigned to PSR varied with ship movement; the latitude and longitude given in Table 1 correspond to the most often assigned grid location while the ship was "on-site." The SOCM(GrADS) land gridpoint information at NZY and CPN represent location and terrain height values for the "second" closest model land gridpoint to the MRS site. The nearest SOCM(GrADS) land gridpoints at NZY and CPN, at very high terrain heights of 266.2 m and 135.9 m, were not used for model M-profiles so as to avoid later comparisons with observed MRS profiles starting at elevations much closer to sea level. For SOCM(GrADS) land point locations, the base (i.e., starting point) of model M-profiles is generally the grid level immediately above the model terrain surface. This model profile base height is 10 m (the first SOCM(GrADS) level above the surface) for CPN, PVN and VBG (before 8/28), 30 m for NZY, 60 m for VBG (from 8/28), and 100 m for NTD; SOCM(GrADS) M-values are available at the NUC land gridpoint at sea level (0 m).

For verification studies, 12 to 24 hour SOCM forecasts (11 to 23 hr for PSR), at 4 hr forecast intervals, will be utilized. With the exception of SOCM initial (0 hr) forecasts (which are used to examine the impact of data assimilation on refractive structure), model forecasts at time periods less than 12 hr (11 hr for PSR) are not used, since such forecasts typically lack sufficient model "spin-up" from initialization. In general, for any MRS sounding at either 00Z or 12Z, SOCM(GrADS) M-profiles at both 12 and 24 hour forecast periods are available for verification; MRS soundings at either 04Z or 16Z, and 20Z, have corresponding model M-profiles at forecast lengths tau= 16 and 20 hours, respectively. In order to preserve correspondence between ship MRS launch times and SOCM data, model M-profiles for the research vessel PSR were extracted from the SOCM(GrADS) database at forecast periods of one hour less than for other sites; these "offtime" forecasts (at tau= 11,15,19 and 23 hr) required an interpolation in time of available SOCM(GrADS) gridded data.

In an analogous procedure as used for the MRS data, SOCM(GrADS) M-profiles were processed to locate all trapping layers between the surface and 1.5 km. All model M-profile trapping layer top and base heights, and their corresponding M-values, were written to data files for subsequent comparison to observed MRS ducting data. Appendix B provides individual station plots of forecast trapping layers at SOCM(GrADS) water gridpoints, at both 12 and

24 hours (11 and 23 hr for PSR). To appear in these plots, a forecast trapping layer must have a thickness > 10 m. This plotting criteria effectively removes all forecast surface (evaporative) ducts of thickness 10 m (as specified by SOCM(GrADS) surface grid resolution), leaving for display only deeper surface ducts. Due to the absence of forecast trapping layers between 1 and 1.5 km, the vertical scale for these station plots does not extend beyond 1 km. SOCM forecasts are plotted according to their verification times in PDT. Trapping layer M-deficits are given by four distinct strength categories; a very weak intensity category (M-unit deficit < 2) is included.

3.3 Spatial and Temporal Variability

In order to examine the spatial and temporal variability of both the VOCAR MRS and SOCM data provided in Appendices A and B, respectively, average trapping layer statistics are computed. These statistics are based on trapping layer heights and intensity of the dominant trapping layer for individual MRS soundings or SOCM(GrADS) M-profiles. Specifically, given all trapping layers of thickness > 10 m from the surface to 1.5 km elevation, the dominant trapping layer for any specified MRS sonde or model profile is chosen as the trapping layer with the largest M-deficit. The requirement that only trapping layers exceeding 10 m thickness are considered in the selection process removes all SOCM(GrADS) water point surface evaporative ducts (of thickness 10 m) from consideration, allowing either a deep surface duct (of thickness $\geq$ 30 m) or an elevated trapping layer to be chosen as the dominant trapping layer for SOCM over water profiles. In rare cases, where 2 or more trapping layers of a MRS sounding have the same maximum M-deficit, the dominant trapping layer is chosen as the one nearest in elevation to the corresponding SOCM dominant trapping layer.

Table 2 presents average VOCAR MRS trapping layer statistics, including those at individual observing sites. The average MRS trapping layer, based on 384 sondes (the NTD sonde of 9/2 12Z did not have a trapping layer of thickness > 10 m), is centered at about 480 m elevation and has a M-gradient near -340 M-units/ km. Trapping layer base and top heights are found to be highest at the MRS sites VBG and NTD, while lowest at San Nicolas Is. and at PSR. On the contrary, the average intensity of the trapping layer (as given by the duct M-deficit, not M-gradient) is weakest at NTD and VBG, and strongest at the NSI and PSR locations (both with deficits > 24 M-units).

Average VOCAR MRS trapping layer heights and intensities, determined for selected observation (launch) times, are presented in Table 3. Here, PSR "offtime" ship launches are grouped with the nearest time category. Excluding the data-deficient 07Z time category

Table 2. Average trapping layer statistics for VOCAR MRS data, including statistics at individual MRS sites.

LOCATION	NO. SONDES	AVERAGE TRAPPING LAYER BASE HEIGHT (m/msl)	TOP HEIGHT (m/msl)	M-DEFICIT (M-units)
	384	449.0	510.3	20.9
NORTH ISLAND(NZY)	50	465.6	536.2	20.0
CAMP PENDLETON(CPN)	53	419.3	508.6	21.3
POINT VICENTE(PVN)	50	456.6	536.3	22.9
POINT MUGU(NTD)	42	493.8	554.1	14.6
VANDENBERG AFB(VBG)	54	522.4	564.1	16.9
SAN CLEMENTE IS.(NUC)	46	489.2	528.7	23.8
SAN NICOLAS IS.(NSI)	55	340.7	395.1	24.1
POINT SUR(PSR)	34	408.7	458.4	24.3

Table 3. Average trapping layer statistics for VOCAR MRS data, at selected observation (launch) times.

	OBSERVATION TIME 07Z	12Z	16Z	20Z	00Z	04Z
AVERAGE TRAPPING LAYER						
BASE HEIGHT (m/msl)	404.2	509.3	515.4	396.3	356.4	462.8
TOP HEIGHT (m/msl)	437.0	574.9	568.2	456.6	419.1	529.7
M-DEFICIT (M-units)	21.2	20.0	17.4	22.2	21.6	23.8
NO. SONDES	5	79	78	69	77	76

(only 5 PSR launches), MRS trapping layer base and top heights show a clear diurnal trend, with highest values near sunrise (12Z to 16Z, sunrise about 1430Z) and lowest trapping layer heights during the late afternoon (00Z). A less sharply defined diurnal trend occurs in trapping layer strength, with weakest trapping occurring in the early morning (16Z) and strongest trapping shortly after sunset (04Z, sunset about 0230Z). From early afternoon (20Z) until evening, the average trapping layer M-deficit remains fairly constant (near 22 M-units).

Average trapping layer statistics corresponding to SOCM(GrADS) 0, 12 and 24 hr water point forecasts are presented in Table 4. At three sites (PVN, NUC and PSR), "dominant" trapping layers were found for all available SOCM(GrADS) 12 and 24 hr forecasts; at NTD, only 19 (18) model forecasts at tau = 0 hr (tau = 24 hr) had either a deep surface (thickness $\geq$ 30 m) or elevated duct. Inspection of Table 4a reveals that, while the average trapping layer base and top heights at MRS locations were generally slightly higher at tau = 0 hr than at tau = 12 hr, they increased considerably over the 12 to 24 hr forecast period (on average, about 100 m in 12 hours). Considerable spatial (site) variability in SOCM(GrADS) average trapping layer height statistics is evident. At NTD, very low average trapping layer heights occur at all forecast lengths, due to a predominance of deep (30 to 60 m thick) surface duct forecasts and a noticeable lack of forecasts of elevated ducting (see NTD plot, Appendix B). These anomalously low trapping layers may reflect model response to complex topography in the vicinity of NTD (e.g., nearby islands). SOCM(GrADS) average trapping layer heights are forecast to be highest at the three offshore sites - NUC, NSI and PSR.

Except for NTD, average forecast trapping layer M-deficits at individual MRS sites are slightly higher at tau = 12 hr than at tau = 0 hr (Table 4b). Overall, the average forecast trapping layer M-deficit decreases only slightly from 12 to 24 hours (19.1 to 17.2 M-units). Over this forecast time interval, average M-deficits decrease at all coastal sites (quite considerably at NZY and CPN) and increase slightly at all offshore sites. SOCM(GrADS) 12 hr average statistics indicate no clear spatial pattern in forecast M-deficit, with values ranging from 25.2 M-units at NTD (large due to many strong surface ducts) to 13.0 M-units at PVN. At tau = 24 hr, a more coherent pattern of spatial variability emerges, with smallest forecast average M-deficits at the southern coastal sites (NZY, PVN and CPN) and largest average M-deficits at the two island locations NUC and NSI. Interestingly, average forecast trapping layer M-deficits at PSR remain considerably below the overall averages at both 12 and 24 hour forecast lengths.

SOCM(GrADS) 0, 12 and 24 hour forecasts can be examined temporally by grouping results into two categories - 00Z and 12Z verification times (Table 5). At all forecast lengths, the strength of the average trapping layer is noticeably less at night (VT 12Z) than at the (day) 00Z verification time. At tau = 24 hr, the average forecast trapping layer base and top heights are much higher at VT 12Z than at VT 00Z (on average, by about 150 m). At both tau = 0 and 12 hr, forecast trapping layer heights are actually somewhat higher at VT 00Z than at VT 12Z.

Table 4. Average trapping layer statistics [(a) base and top heights, (b) M-deficit] for SOCM(GrADS) 0, 12 and 24 hr water point forecasts, including statistics for individual MRS sites.

(a) Base and Top Heights

		TAU= 0 HR		TAU=12 HR		TAU=24 HR	
		AVERAGE TRAPPING LAYER					
SITE	NO.FCST	BASE HGT (m/msl)	TOP HGT (m/msl)	BASE HGT (m/msl)	TOP HGT (m/msl)	BASE HGT (m/msl)	TOP HGT (m/msl)
	148	184.4	318.7				
	164			178.4	314.1		
	161					270.4	414.3
NZY	21,21,21	170.2	277.6	167.9	277.6	274.3	390.7
CPN	21,21,21	161.9	280.7	151.2	269.1	289.3	398.1
PVN	22,23,23	197.3	358.0	188.0	342.4	256.5	410.9
NTD	19,21,18	27.6	76.8	25.0	72.4	97.2	158.9
VBG	22,22,21	170.2	313.6	155.2	305.9	236.4	386.9
NUC	22,23,23	271.6	444.3	264.1	437.0	341.7	531.5
NSI	21,21,22	272.6	448.8	254.8	429.8	347.1	543.2
PSR	---,12,12	-----	-----	238.3	402.1	298.8	460.4

(b) M-Deficit

		TAU= 0 HR	TAU=12 HR	TAU=24 HR
SITE	NO. FCST	AVERAGE TRAPPING LAYER M-DEFICIT (M-units)		
	148	18.7		
	164		19.1	
	161			17.2
NZY	21,21,21	18.6	19.3	12.8
CPN	21,21,21	20.4	22.1	14.0
PVN	22,23,23	12.9	13.0	12.9
NTD	19,21,18	27.6	25.2	21.8
VBG	22,22,21	13.5	15.6	15.3
NUC	22,23,23	20.7	21.9	23.0
NSI	21,21,22	18.8	20.1	22.3
PSR	---,12,12	----	14.1	14.6

Table 5. Average trapping layer statistics for SOCM(GrADS) 0, 12 and 24 hr water point forecasts, at 00Z and 12Z verification times.

		VT 00Z			VT 12Z		
		AVERAGE TRAPPING LAYER					
FCST TAU	NO. FCST	BASE HGT (m/msl)	TOP HGT (m/msl)	M-DEF. (M-units)	BASE HGT (m/msl)	TOP HGT (m/msl)	M-DEF. (M-units)
0HR	76,72	194.5	336.3	20.5	173.7	300.0	16.9
12HR	82,82	196.5	344.4	21.1	160.2	283.7	17.1
24HR	86,75	195.6	341.1	19.6	356.1	498.2	14.4

Interestingly, while average trapping layer height statistics at the 00Z verification time are remarkable similar at the 0, 12 and 24 hr forecast lengths, statistics for forecasts verifying at 12Z indicate a large rise (of about 200 m) in average trapping layer height over the 12 to 24 hour forecast period.

Inspection of MRS and SOCM(GrADS) individual station plots given in Appendices A and B strongly suggests that synoptic (large-scale) variability was significant within the VOCAR study area during the summer 1993 intensive observing period. To examine this further, composite time series of average trapping layer height and strength were computed for both MRS observations and SOCM(GrADS) 12 and 24 hr water point forecasts (validated at MRS sites). All time series originally contain 23 points at 12 hr intervals, with each individual (time) point corresponding to the composite (average) of all available MRS observations (or SOCM forecasts) at that particular time. A single pass of a 1-2-1 filter is applied to all original series to remove high frequency (i.e., diurnal) variations. Resultant filtered time series (of length 21 points) are shown in Figure 3 ; thin horizontal lines represent means of individual time series.

Both observed and forecast trapping layer base and top heights (Figs. 3a and 3b, respectively) exhibit considerable variability, with generally two periods each of high and low trapping layer heights during the full 11 day observing period. Visual comparisons among curve peaks and troughs indicate that observed and forecast trapping layer heights are typically out of phase by 1/2 to 1 1/2 days. Although difficult to quantify (due to short time series length), the time scale of both observed and forecast synoptic fluctuations in trapping layer height appears to be about 5 to 7 days. The filtered time series of observed trapping layer M-deficit (Fig. 3c) indicates large values (generally above 30 M-units) before August 28, a rapid decrease over mid period, and fairly steady M-deficits (below 10 M-units) during the last few observing days.

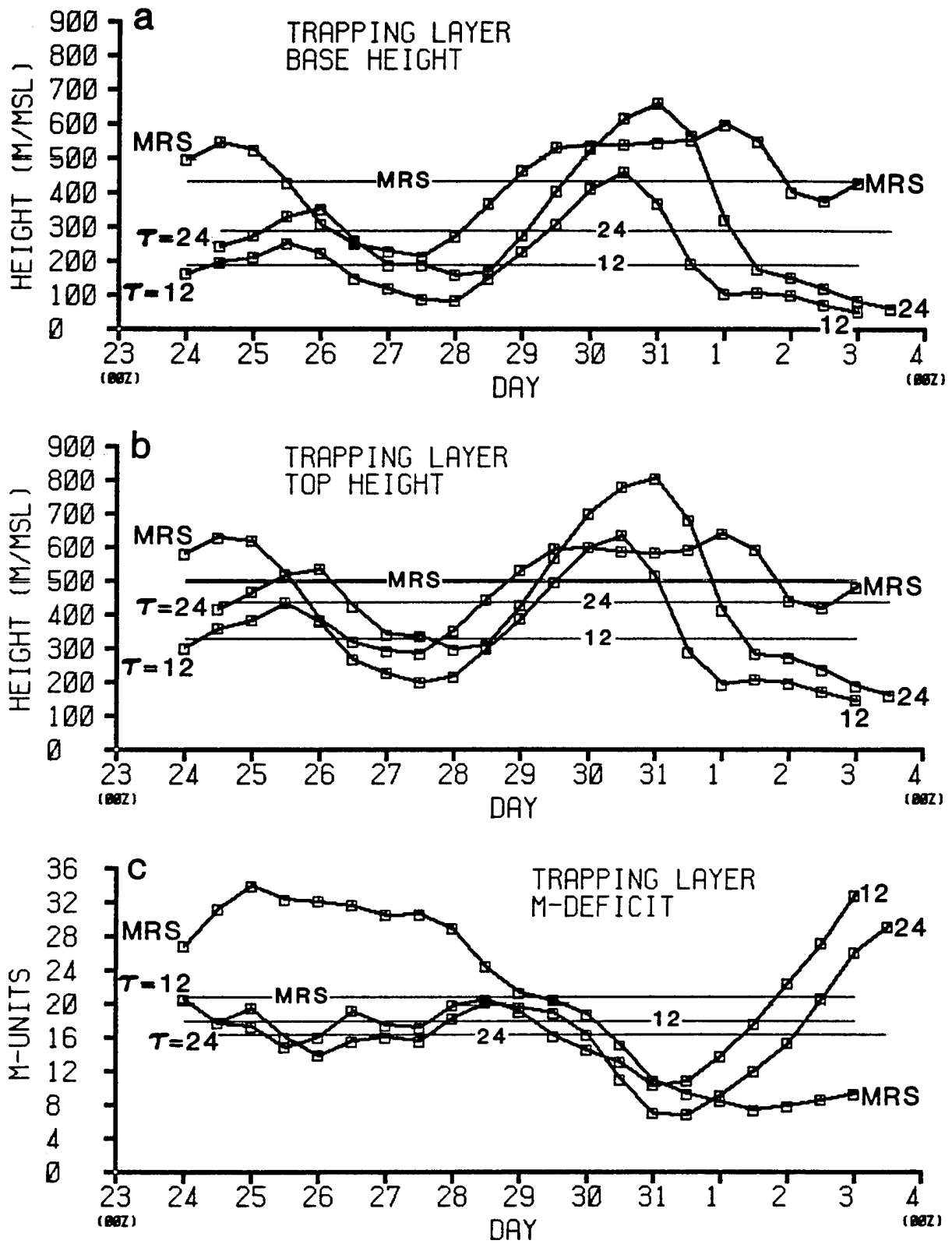

Figure 3. Low-pass filtered composite time series of trapping layer base height (a), top height (b) and M-deficit (c) during the VOCAR summer 1993 experiment, for MRS observations and SOCM(GrADS) 12 and 24 hr water point forecasts. Means of individual time series are also displayed.

Forecast 12 and 24 hr M-deficits exhibit only slight fluctuations about their means (18 and 16.4 M-units, respectively) over the first half of the observing period, then decrease steadily to minimums on August 31 before intensifying rapidly to maximum values near 30 M-units by the end of the observing period. Over the second half of the observing period, a strong negative correlation is apparent between (filtered) time series of forecast trapping layer height and forecast M-deficit.

4. MODEL INITIALIZATION

For the VOCAR experiment, SOCM was run with a 12 hr incremental update procedure which consisted of two basic steps - data analysis and initialization. At the start of each model forecast, a MVOI analysis was performed to update first guess, or background, fields using "current" observations available within the FNMOC operational database. Except for the initial SOCM forecast (at 8/23 00Z start time), the analysis first guess fields (FGF) were 12 hr forecast fields valid at the analysis time made by the mesoscale (SOCM) forecast model. Following the analysis, a NLVMI scheme was used to adjust (by removing gravity wave noise) the analyzed fields prior to their use as initial conditions by the forecast model. According to Goerss and Phoebus (1993), if the analysis is performed in an effective manner, the initialization will only make small adjustments to these fields. Based on this assertion, SOCM refractivity fields after model initialization (i.e., at tau = 0 hr) will be considered as "analysis" fields.

In order to examine the impact of data assimilation on refractive structure, direct comparisons are made between SOCM analysis (tau = 0 hr) and corresponding background (12 hr forecasts valid at the analysis time) refractivity profiles. Table 6 provides analysis minus first guess field (ANL - FGF) statistics for trapping layer base and top heights and M-deficit, corresponding to both SOCM(GrADS) water and land point forecasts. These statistics are based on 148 (122) over water (over land) (ANL - FGF) data. Both sets of statistics do not include data for the research vessel PSR; in addition, the over land statistics lack data at NSI. Taken collectively, statistical results shown in Table 6 indicate small differences between background and analysis trapping layer characteristics. For both land and water point forecasts, M-deficit mean deviations indicate trapping layer strength to be only slightly higher for background M-profiles than those subsequent to analysis. Analysis minus background mean differences for trapping layer top and bottom heights are several meters. Interestingly, for water point forecasts,

Table 6. Analysis minus background (first guess field) mean deviation (MD), absolute mean deviation (AMD) and root mean square difference (RMSD) statistics for trapping layer base and top heights and M-deficit, corresponding to SOCM(GrADS) water and land point forecasts.

PREDICTOR	SOCM WATER PT. FCST			SOCM LAND PT. FCST		
STATISTIC	MD	AMD	RMSD	MD	AMD	RMSD
TRAPPING LAYER						
BASE HEIGHT (m)	7.1	7.1	27.5	-2.3	12.1	51.7
TOP HEIGHT (m)	6.2	6.2	33.4	-3.6	11.0	59.5
M-DEFICIT (M-units)	-1.1	2.1	3.9	-0.5	1.0	2.0

the mean and absolute mean height deviations are the same, indicating that all (ANL - FGF) differences are positive. While Table 6 RMS differences for trapping layer heights are considerably larger than mean deviations, they are still roughly an order of magnitude less than forecast minus observed trapping layer height RMS differences discussed later in the report (in Section 5.2).

To further quantify analysis minus background M-profile differences, trapping layer top and bottom height limits were examined. Of the 270 combined water and land point data used for Table 6, almost 88% of the data had background and analysis M-profiles with identical bottom and top trapping layer heights, another 10% had overlapping dominant trapping layers (usually with only one height limit different) and only about 2% (6 data - 3 each for land and water locations) had distinct background and analysis dominant trapping layers. If not for these several occurrences of distinct, non-matching background and analysis trapping layers, Table 6 mean and absolute mean deviations would have been even smaller, and RMS differences considerably smaller.

Various factors could have been responsible for the generally limited impact of data assimilation on refractive structure during model initialization. First, the MVOI analysis step could have been done in a computationally erroneous manner - this does not seem to have occurred. Second, the data assimilation cycle perhaps had a limited effect due to a pronounced and consistent lack of observational data during the VOCAR forecast period. A check of the FNMOC database archives indicates that a decent coverage of upper air and surface data was

available within the VOCAR model domain throughout the summer 1993 intensive observing period. Information provided in Figure 1 indicates that, for each of the 25 model runs made for VOCAR, typically about a dozen conventional radiosondes were available within the SOCM grid domain for data assimilation. Within the Southern California bight region, routine synoptic (00Z and 12Z) radiosondes were almost always available for SOCM data assimilation at or near two MRS sites (Montgomery Field (near North Island) and Vandenberg AFB) and often available at two other sites (Pt. Mugu and San Nicholas Is.). Third, the vertical data resolution of the MVOI analysis was inadequate for updating model background fields - this factor is believed to have been very critical. Generally, within the boundary layer below 850 mb (~1.5 km), the MVOI provides updated information to first guess fields at only 3 levels (1000, 925 and 850 mb). An analysis of such low vertical resolution is likely to smooth, or miss entirely, important refractive (i.e. inversion) layers of shallow depth (usually reported by conventional radiosondes as significant levels), thus providing little significant adjustment to the shape of model background profiles of much higher resolution (i.e., 15 levels below 850 mb). Finally, the MVOI scheme does not analyze moisture, which is the most dominant factor in defining refractive structure. Without any moisture information, modifications to model-derived background refractivity profiles (via the temperature field alone) during the analysis process are clearly limited.

5. COMPARISON RESULTS

In this study, an assessment of SOCM's ability to forecast refractive structure (viz. ducting) is made by direct comparisons between model and observed (MRS) refractivity profiles. SOCM water and land point forecasts are compared in order to assess the degree of importance of model terrain type in forecasting performance. Comparison results for duct occurrence are based on simple contingency table statistical indices, while average error statistics are used for verification of trapping layer height and intensity. Statistics are computed for 12 to 24 hr forecast lengths at intervals of 4 hr, and include "offtime" PSR ship data (grouped with the nearest time category). SOCM forecasting performance at diurnal and synoptic time scales is also examined in this section.

5.1 Duct Occurrence

Performance statistics for the occurrence of ducting are computed for both surface and elevated ducts. A surface duct will be considered to occur for any profile (radiosonde or model-derived) with a surface or surface-based (from an elevated trapping layer) duct of thickness $\geq$ 30 m and M-deficit $\geq$ 2 M-units. Overall, slightly less than 20% of MRS soundings have surface ducts which meet these criteria. The requirement for a duct thickness $\geq$ 30 m eliminates many shallow surface ducts (including SOCM(GrADS) water point evaporative ducts of thickness 10 m), thus providing for performance assessment of only significantly deep surface ducts. The assessment of elevated ducting is based on the occurrence of elevated trapping layers. Specifically, an elevated trapping layer will be considered to occur for any profile (MRS or model-derived) with at least one elevated trapping layer of thickness $\geq$10 m and M-deficit $\geq$ 2 M-units within 1.5 km of the surface. Overall, only five MRS soundings did not meet these criteria for elevated trapping layer occurrence.

Surface ducting statistical indices (the prefigurance , postagreement, percent correct and false alarm rate)* for SOCM(GrADS) water and land point forecasts are given in Table 7. Postagreement values (which measure forecast reliability) are generally near 0.2, while scores for prefigurance are considerably higher, ranging from about 1/3 to 1/2. Note that the number of SOCM surface duct forecasts is considerably higher over water than land, at all forecast lengths. For either the PF or PA index, no significant differences in scores are noted between SOCM water and land point forecasts. At all forecast lengths, SOCM land point forecasts have better PC and FAR (the lower the score, the better) scores than comparable SOCM water point forecasts, with differences in scores greatest at tau = 12 hr. Except for the PF index, both SOCM predictors have better performance scores at tau = 24 hr than at tau = 12 hr; for the PC and FAR indices, this improvement results largely from a significant decrease in the number of erroneous surface duct forecasts (and a corresponding increase in correct forecasts of no ducting occurrences).

---

*Given a particular event (i.e., surface ducting),

PF(prefigurance)	=	no. of correct forecasts / no. observed,
PA(postagreement)	=	no. of correct forecasts / no. of forecasts issued ,
PC(percent correct)	=	no. of correct forecasts (events and non-events) / total no. of events and non-events, multiplied by 100 , and
FAR(false alarm rate)	=	no. of incorrect forecasts / no. of non-events observed.

Table 7. Surface ducting performance statistics for SOCM(GrADS) water and land point 12 to 24 hr forecasts, during the VOCAR summer 1993 intensive observing period.

PREDICTOR	TAU=12	TAU=16	TAU=20	TAU=24
		PREFIGURANCE (PF)		
SOCM W.PT.	15/29=.517	15/34=.441	5/11=.455	10/29=.345
SOCM L.PT.	9/19=.474	9/25=.360	3/6=.500	7/19=.368
		POSTAGREEMENT (PA)		
SOCM W.PT.	15/85=.176	15/63=.238	5/33=.152	10/53=.189
SOCM L.PT.	9/46=.196	9/40=.225	3/18=.167	7/31=.226
		PERCENT CORRECT (PC/100)		
SOCM W.PT.	73/157=.465	87/154=.565	40/74=.541	94/156=.603
SOCM L.PT.	77/124=.621	74/121=.612	33/51=.647	87/123=.707
		FALSE ALARM RATE (FAR)		
SOCM W.PT.	70/128=.547	48/120=.400	28/63=.444	43/127=.339
SOCM L.PT.	37/105=.352	31/96=.323	15/45=.333	24/104=.231

Elevated trapping layer performance statistics for SOCM water and land point forecasts are presented in Table 8. Here, the FAR index is not given due to a statistically insignificant number of observed no trapping occurrences (3 at 12Z, one each at 16Z and 00Z). Given the extremely high incidence of both observed and forecast elevated trapping layers, all post-agreement scores are at, or very near, one. For a specific predictor and forecast tau, PF and PC scores are identical (at tau = 20 hr) or nearly identical. At tau = 12, 16 and 24 hr, PF and PC scores corresponding to SOCM water forecasts are significantly higher (by about 0.2) than comparable scores for SOCM land point forecasts. These higher PF and PC scores for SOCM water point forecasts (compared to land forecasts) result from a significantly larger number of correct elevated trapping layer forecasts combined with a smaller number of incorrect forecasts (the latter in spite of a larger SOCM over water data sample). Finally, for either SOCM predictor, little numerical difference is observed in elevated trapping layer performance statistics at the 12 and 24 hr forecast lengths.

Table 8. Elevated trapping layer performance statistics for SOCM(GrADS) water and land point 12 to 24 hr forecasts, during the VOCAR summer 1993 intensive observing period.

PREDICTOR	TAU=12	TAU=16	TAU=20	TAU=24
		PREFIGURANCE (PF)		
SOCM W.PT.	124/153=.810	118/153=.771	63/74=.851	123/152=.809
SOCM L.PT.	74/121=.612	68/120=.567	40/51=.784	75/120=.625
		POSTAGREEMENT (PA)		
SOCM W.PT.	124/126=.984	118/118= 1.0	63/63= 1.0	123/126=.976
SOCM L.PT.	74/75=.987	68/69=.986	40/40= 1.0	75/76=.987
		PERCENT CORRECT (PC/100)		
SOCM W.PT.	126/157=.803	119/154=.773	63/74=.851	124/156=.795
SOCM L.PT.	76/124=.613	68/121=.562	40/51=.784	77/123=.626

Table 9 presents surface ducting performance statistics for SOCM(GrADS) water and land point 12 and 24 hr forecasts based on day (VT 00Z) and night (VT 12Z) categories. For both 12 and 24 hr forecasts, the PF and PA indices for both SOCM predictors are higher at VT 00Z than at VT 12Z ; the largest of these day-night differences (the PF score at tau = 24 hr) is enhanced due to a very good forecast capability at VT 00Z and a nil capability (for both predictors) at VT 12Z. On the contrary, PC and FAR scores for both SOCM predictors are better at night (VT 12Z); at tau = 24 hr, SOCM water and land point FAR VT 12Z scores are much lower than those at 00Z (note the substantially fewer number of incorrect surface duct forecasts). Based on day-night categories, all performance statistics for SOCM land point forecasts are better than comparable water point forecasts with the exception of the PF and PA indices at VT 12Z. In general, daytime (VT 00Z) statistics indicate a slight improvement in surface ducting forecasting performance from the 12 to 24 hr forecast interval; on the other hand, SOCM nighttime (VT 12Z) PF and PA indices fall, while PC and FAR scores improve, over this 12 hour forecast period. The most noticeable difference in SOCM 24 hr forecasts (when compared to 12 hr forecasts) is the sharp decline in the number of forecasts of surface ducting at VT 12Z.

Elevated trapping layer day (VT 00Z) and night (VT 12Z) performance statistics for the SOCM(GrADS) predictors are given in Table 10. At both the 12 and 24 hr forecast lengths, all statistical indices for both SOCM predictors are higher at VT 00Z than at VT 12Z. Day-night score differences are generally not large, except for the SOCM(GrADS) land point PF and PC

Table 9. Surface ducting performance statistics for SOCM(GrADS) water and land point 12 and 24 hr forecasts, based on day (VT 00Z) and night (VT 12Z) data subsets.

	TAU = 12 HR		TAU = 24 HR	
PREDICTOR	VT 00Z	VT 12Z	VT 00Z	VT 12Z
		PREFIGURANCE (PF)		
SOCM W.PT.	9/16=.563	6/13=.462	10/16=.625	0/13= 0.0
SOCM L.PT.	6/10=.600	3/9=.333	7/10=.700	0/9= 0.0
		POSTAGREEMENT (PA)		
SOCM W.PT.	9/46=.196	6/39=.154	10/41=.244	0/12= 0.0
SOCM L.PT.	6/26=.231	3/20=.150	7/27=.259	0/4= 0.0
		PERCENT CORRECT (PC/100)		
SOCM W.PT.	33/77=.429	40/80=.500	40/77=.519	54/79=.684
SOCM L.PT.	37/61=.607	40/63=.635	38/61=.623	49/62=.790
		FALSE ALARM RATE (FAR)		
SOCM W.PT.	37/61=.607	33/67=.493	31/61=.508	12/66=.182
SOCM L.PT.	20/51=.392	17/54=.315	20/51=.392	4/53=.075

Table 10. Elevated trapping layer performance statistics for SOCM(GrADS) water and land point 12 and 24 hr forecasts, based on day (VT 00Z) and night (VT 12Z) data subsets.

	TAU = 12 HR		TAU = 24 HR	
PREDICTOR	VT 00Z	VT 12Z	VT 00Z	VT 12Z
		PREFIGURANCE (PF)		
SOCM W.PT.	65/76=.855	59/77=.766	62/76=.816	61/76=.803
SOCM L.PT.	47/61=.770	27/60=.450	41/61=.672	34/59=.576
		POSTAGREEMENT (PA)		
SOCM W.PT.	65/66=.985	59/60=.983	62/63=.984	61/63=.968
SOCM L.PT.	47/47= 1.0	27/28=.964	41/41= 1.0	34/35=.971
		PERCENT CORRECT (PC/100)		
SOCM W.PT.	65/77=.844	61/80=.763	62/77=.805	62/79=.785
SOCM L.PT.	47/61=.770	29/63=.460	41/61=.672	36/62=.581

indices at tau = 12 hr; here, substantially fewer nighttime (VT 12Z) trapping forecasts (about 20 less) results in significantly lower PF and PC scores than at VT 00Z. While little difference in PA scores are noted between the two SOCM predictors (both near or equal to 1), SOCM (GrADS) water point forecasts yield higher PF and PC scores than SOCM(GrADS) land point forecasts; PF and PC score differences between SOCM predictors exceed 0.3 at tau = 12, VT 12Z. Finally, while SOCM(GrADS) PF and PC nighttime (VT 12Z) scores improved slightly from tau = 12 hr to tau = 24 hr, analogous scores at VT 00Z decreased slightly over this forecast interval; in all cases, 12 to 24 hour score differences are not significant.

5.2 Trapping Layer Height and Intensity

Average error statistics used for verification of trapping layer height and intensity are based on differences between observed (MRS) and predicted (SOCM) trapping layer characteristics. Forecast minus observed differences are computed provided that both the radiosonde and corresponding SOCM water or land M-profile have "dominant" trapping layers of thickness >10 m within 1.5 km of the surface. As discussed previously, the "dominant" trapping layer of a MRS sonde or model profile is chosen as the trapping layer (surface or elevated) with the largest M-deficit.

Table 11 gives the SOCM(GrADS) bias, mean absolute error (MAE) and root mean square error (RMSE) 12 to 24 hr statistics for trapping layer base and top heights and intensity, based on all available data. Model biases for trapping layer top and bottom heights are all negative, indicating a tendency to underforecast. Average magnitudes of trapping layer height biases mostly exceed 150 m; except at tau = 12 hr, bias magnitudes are somewhat greater for SOCM land point forecasts. The average magnitude of forecast errors (as given by the MAE and RMSE statistics) is large for trapping layer heights, generally a few hundred meters. SOCM(GrADS) trapping layer M-deficits biases are negative at all forecast lengths. The underforecasting of trapping layer strength is more pronounced with SOCM land point forecasts (as opposed to SOCM water point forecasts); in spite of this, both MAE and RMSE statistics are comparable for both SOCM predictors. Trapping layer M-deficit MAE and RMSE statistics are large for all predictors, with RMSE values being comparable in magnitude to the overall average observed MRS M-deficit (20.9 M-units). Although error statistics presented in Table 11 do not indicate a clear trend in SOCM forecasting skill over the 12 to 24 hour interval, a comparison of only 12 and 24 hr error statistics suggests that, on average, SOCM trapping layer height and intensity forecasts at 24 hr are somewhat more accurate than those at 12 hr.

Table 11. Bias, mean absolute error and root mean square error statistics for trapping layer base and top heights and M-deficit, derived from SOCM(GrADS) water and land point forecasts, at tau = 12, 16, 20 and 24 hr.

		TAU=12	TAU=16	TAU=20	TAU=24
TRAPPING LAYER BASE HEIGHT (m)					
BIAS	SOCM WATER PT.	-250.2	-250.1	-159.0	-151.7
	SOCM LAND PT.	-225.8	-283.3	-225.0	-173.6
MAE	SOCM WATER PT.	288.0	301.3	236.4	245.4
	SOCM LAND PT.	286.8	308.4	249.3	254.7
RMSE	SOCM WATER PT.	367.3	385.8	288.5	322.4
	SOCM LAND PT.	364.7	385.2	287.4	332.4
TRAPPING LAYER TOP HEIGHT (m)					
BIAS	SOCM WATER PT.	-178.8	-175.2	- 55.1	-69.4
	SOCM LAND PT.	-169.4	-217.4	-154.8	-93.1
MAE	SOCM WATER PT.	264.6	281.0	209.9	237.7
	SOCM LAND PT	264.3	271.2	217.5	241.0
RMSE	SOCM WATER PT.	346.9	361.4	267.3	316.9
	SOCM LAND PT.	347.5	349.0	262.3	322.5
TRAPPING LAYER M-DEFICIT (M-units)					
BIAS	SOCM WATER PT.	-2.8	-4.5	-7.3	-5.3
	SOCM LAND PT.	-11.3	-10.2	-10.9	-10.5
MAE	SOCM WATER PT.	15.5	14.3	15.7	13.6
	SOCM LAND PT.	14.3	14.6	16.2	13.9
RMSE	SOCM WATER PT.	19.7	18.2	21.1	17.8
	SOCM LAND PT.	19.2	19.5	23.9	18.3

Results shown in Table 11 are based on unequal numbers of forecast/observation pairs among predictors. In order to more accurately compare forecast performance among predictors, error statistics based on coincidental predictions were computed (Table 12). These statistics are based on a total of 110, 96, 46 and 97 coincidental forecasts, at tau = 12, 16, 20 and 24 hr, respectively. Missing forecasts at NSI and PSR (only water point forecasts) account for much of the decrease in sample size (from the full data set); sample size differences between tau = 12 hr, and tau = 16 and 24 hr, are due largely to a decrease in the number of SOCM(GrADS) land point forecasts with trapping layers after 12 hours.

Table 12. Bias, mean absolute error and root mean square error statistics for trapping layer base and top heights and M-deficit, derived from coincidental SOCM(GrADS) water and land point forecasts, at tau= 12, 16, 20 and 24 hr.

		TAU=12	TAU=16	TAU=20	TAU=24
TRAPPING LAYER BASE HEIGHT (m)					
BIAS	SOCM WATER PT.	-268.1	-298.6	-242.4	-192.3
	SOCM LAND PT.	-234.1	-286.8	-225.0	-170.1
MAE	SOCM WATER PT.	306.2	319.2	264.5	271.3
	SOCM LAND PT.	283.2	311.2	249.3	252.1
RMSE	SOCM WATER PT.	383.1	404.2	306.4	344.9
	SOCM LAND PT.	360.4	388.4	287.4	330.0
TRAPPING LAYER TOP HEIGHT (m)					
BIAS	SOCM WATER PT.	-200.4	-234.2	-147.4	-113.1
	SOCM LAND PT.	-178.0	-218.9	-154.8	-89.6
MAE	SOCM WATER PT.	280.4	287.5	205.9	252.3
	SOCM LAND PT	259.7	273.9	217.5	239.0
RMSE	SOCM WATER PT.	361.8	372.8	255.1	331.6
	SOCM LAND PT.	341.1	351.7	262.3	321.2
TRAPPING LAYER M-DEFICIT (M-units)					
BIAS	SOCM WATER PT.	-1.2	-2.8	-7.2	-3.6
	SOCM LAND PT.	-11.5	- 9.8	-10.9	-10.6
MAE	SOCM WATER PT.	15.2	13.8	16.8	13.3
	SOCM LAND PT.	14.4	14.3	16.2	14.0
RMSE	SOCM WATER PT.	19.7	18.0	23.1	17.5
	SOCM LAND PT.	19.3	18.8	23.9	18.4

In spite of about a one third reduction in sample size, performance statistics for coincidental comparisons given in Table 12 are not greatly different from results examined previously for the full data set. While comparisons of SOCM water and land point error statistics of Table 12 indicate overall better performance for land-based forecasts of trapping layer heights, differences between the two SOCM predictors are not significant. Regarding these comparisons, recall that SOCM(GrADS) land point M-profiles typically start above sea level; as a consequence, any SOCM surface trapping layer over land is "elevated" somewhat compared to an analogous

SOCM over water surface trapping layer, and often is closer in height to the observed trapping layer. Over the 12 to 24 hr forecast interval, the magnitudes of M-deficit biases for SOCM water point forecasts average 3.7 M-units; with generally weaker trapping layers, M-deficit biases for the SOCM land point predictor are considerably higher. For any selected trapping layer characteristic (height or intensity) and statistic (bias, MAE or RMSE), no predictor shows a steady (monotonically increasing or decreasing) trend over the 12 to 24 hr forecast period, when examined at 4 hr forecast increments. However, comparisons of SOCM water and land point error statistics at 12 and 24 hr forecast lengths (based on much the same MRS data) indicate better model performance at tau = 24 hr, with only one statistical value (the SOCM water point predictor's M-deficit bias) slightly better at tau = 12 hr.

In order to examine diurnal variability in prediction of trapping layer height and intensity, average error statistics were computed for SOCM 12 and 24 hr forecasts based on day (VT 00Z) and night (VT 12Z) categories (Table 13). At tau = 12 hr, all SOCM water and land point error statistics for trapping layer base and top heights are considerably better during the day than at night. The large day-night differences in bias at tau = 12 hr are a result of both a lower average model trapping layer height and a higher average observed (MRS) height, at VT 12Z (compared to VT 00Z). SOCM error statistics for trapping layer heights at tau = 24 hr do not indicate a distinct difference in day and night forecasts, although many error statistics are better at VT 00Z. At both the 12 and 24 hr forecast lengths, all trapping layer M-deficit error statistics for the SOCM(GrADS) over water predictor are better at VT 00Z than at VT 12Z, with day-night error differences less pronounced at tau = 24 hr.

As previously discussed in Section 3.3, both observed and model (SOCM) data exhibited considerable large-scale variability during the summer 1993 VOCAR experiment. A comparison of forecast and observed synoptic trends (Figure 3) indicates that, while the model was quite successful in forecasting the trend toward a higher trapping layer of diminished intensity during the middle of the VOCAR observing period (i.e., the last few days of August), it fared considerably worse at both the beginning and end of the observing period. While inadequacies in SOCM physics are likely the key factor in faulty forecasting performance, other factors (such as inaccurate time-dependent boundary conditions and insufficient model updating during analysis) may be important.

Table 13. Day (VT 00Z) and night (VT 12Z) bias, mean absolute error and root mean square error statistics for trapping layer base and top heights and M-deficit, derived from SOCM (GrADS) water and land point forecasts, at tau = 12 and 24 hr.

		TAU = 12 HR		TAU = 24 HR	
		VT 00Z	VT 12Z	VT 00Z	VT 12Z
TRAPPING LAYER BASE HEIGHT (m)					
BIAS	SOCM WATER PT.	-159.9	-344.2	-155.9	-147.4
	SOCM LAND PT.	-144.9	-317.6	-141.3	-211.6
MAE	SOCM WATER PT.	231.5	346.9	235.1	256.0
	SOCM LAND PT.	229.4	351.9	233.2	280.1
RMSE	SOCM WATER PT.	315.0	414.8	319.2	325.8
	SOCM LAND PT.	309.4	418.7	311.1	355.9
TRAPPING LAYER TOP HEIGHT (m)					
BIAS	SOCM WATER PT.	-77.6	-284.3	-74.0	-64.6
	SOCM LAND PT.	-81.1	-269.6	-60.4	-131.6
MAE	SOCM WATER PT.	228.4	302.2	237.6	237.8
	SOCM LAND PT.	218.6	316.2	236.7	246.0
RMSE	SOCM WATER PT.	317.6	374.9	328.0	304.8
	SOCM LAND PT.	304.5	390.6	322.6	322.5
TRAPPING LAYER M-DEFICIT (M-units)					
BIAS	SOCM WATER PT.	-0.5	-5.1	-3.8	-6.8
	SOCM LAND PT.	-9.8	-13.1	-10.4	-10.7
MAE	SOCM WATER PT.	14.3	16.8	13.3	14.1
	SOCM LAND PT.	13.4	15.3	14.4	13.2
RMSE	SOCM WATER PT.	18.7	20.7	17.6	17.9
	SOCM LAND PT.	18.7	19.8	19.0	17.5

Quantitatively, SOCM's ability to forecast synoptic trends will be examined against 12 hr trend persistence forecasts computed from the Figure 3 low-pass filtered time series representing (after removal of series means) observed synoptic trends in trapping layer height and intensity. For a given parameter (trapping layer height or M-deficit), a 12 hr persistence forecast is obtained by adding the (signed) difference in observed values over the previous 12 hours to the current observed value of the chosen parameter. Given the length and step increment (12 hr) of the Figure 3 time series, a total of 19 individual persistence forecasts were made for each trapping layer parameter, starting at 8/25 00Z and ending 9/3 00Z.

A comparison of observed and forecast mean values presented in Figure 3 indicates that, on average, SOCM (most especially at the 12 hr forecast length) significantly underforecasts both trapping layer height and intensity. In order to more fairly compare 12 hr persistence forecasts (which closely track the observed) with SOCM forecasts, error statistics will not be computed using actual (forecast - observed) differences in the synoptic "signal" but rather will be derived from (forecast - observed) differences in 12 hr synoptic trend. Table 14 gives the percent of time each chosen predictor (12 hr persistence, SOCM(GrADS) 12 and 24 hr forecasts) correctly forecast the observed 12 hr synoptic trend (upwards or downwards) in trapping layer base and top heights and intensity. Results show that, for all trapping layer parameters, 12 hr persistence was more often able to correctly forecast synoptic trends than either SOCM(GrADS) 12 or 24 hr forecasts. On average, 12 hr persistence was able to predict correctly synoptic trends in trapping layer height and intensity about 75% of the time, while SOCM (12 and 24 hr forecasts combined) correctly forecast large-scale trends about 3 out of every 5 times. All average error statistics derived from (forecast-observed) differences in 12 hr synoptic trend (Table 15) indicate better forecast performance for 12 hr persistence than for SOCM. For trapping layer base and top height, Table 15 results show better bias, MAE and RMSE statistics for SOCM 12 hr forecasts than for 24 hr forecasts; on the contrary, SOCM error statistics for the synoptic trend in trapping layer intensity (M-deficit) are slightly better at the longer forecast interval.

6. SUMMARY AND CONCLUSIONS

In support of the VOCAR experiment conducted from August 23 to September 3, 1993 in the Southern California bight region, 24 hr forecasts from a second order closure R&D version of NORAPS (SOCM) were made every 12 hours at the FNMOC for the VOCAR domain. This report serves as a validation of SOCM's capabilities in short-range forecasting of lower tropospheric ducting during the VOCAR experiment. For verification, direct comparisons of refractive structure were made among SOCM 12 to 24 hr forecasts, and high resolution coastal, island and ship miniradiosondes launched throughout the intensive observing period. Various statistical indices, derived from forecast/observed contingency tables, were used to assess SOCM's ability to forecast both surface and elevated ducting. The accuracy of SOCM duct height and intensity forecasts were evaluated using average error statistics. SOCM forecasting performance at both diurnal and synoptic time scales and, over both water and land surfaces,

Table 14. Percent of time selected predictors (Persistence, SOCM(GrADS) 12 and 24 hr water point forecasts) correctly forecast the observed 12 hr large-scale synoptic trend in trapping layer height and intensity during the summer 1993 VOCAR experiment. Data were extracted from Fig. 3 time series.

	PERSISTENCE	SOCM 12 hr FCST	SOCM 24 hr FCST
TRAPPING LAYER			
BASE HEIGHT	15/19 78.9%	12/20 60.0%	12/19 63.2%
TOP HEIGHT	13/19 68.4%	13/20 65.0%	10/19 52.6%
M-DEFICIT	15/19 78.9%	10/20 50.0%	12/19 63.2%

Table 15. Bias, MAE and RMSE statistics for trapping layer base and top heights and M-deficit, derived from forecast minus observed differences in 12 hr synoptic trend. Statistics are based on Fig. 3 time series data and, 19 coincidental forecasts from three predictors - 12 hr persistence, and 12 and 24 hr SOCM(GrADS) water point forecasts.

	12 hr PERSISTENCE	SOCM 12 hr FCST	SOCM 24 hr FCST
TRAPPING LAYER BASE HEIGHT (m)			
BIAS	-0.1	-1.5	-2.2
MAE	48.8	66.1	86.8
RMSE	61.0	84.2	108.0
TRAPPING LAYER TOP HEIGHT (m)			
BIAS	-0.6	-3.3	-4.1
MAE	52.0	73.1	95.4
RMSE	63.1	94.4	117.3
TRAPPING LAYER M-DEFICIT (M-units)			
BIAS	+0.2	+2.0	+1.6
MAE	1.4	2.7	2.4
RMSE	1.8	3.2	3.0

were examined. In order to assess the impact of data assimilation with an incremental update procedure on refractive structure, direct comparisons were made between SOCM first guess and analysis trapping layer parameters.

Of the nearly 400 miniradiosondes utilized for this study, all but one (i.e., 99.7%) had at least one trapping layer of thickness > 10 m within 1.5 km of the surface. During the VOCAR experiment, average trapping layer heights were highest at Point Mugu (NTD) and Vandenberg AFB (VBG) and lowest at San Nicolas Is. (NSI) and with the Point Sur research vessel (PSR). On the contrary, average observed trapping layer intensities (i.e., M-deficits) were weakest at NTD and VBG and strongest at NSI and PSR. When averaged according to observation (i.e., launch) time, MRS trapping layer base and top heights show a clear diurnal trend, with highest values near sunrise and lowest heights during the late afternoon. A less sharply defined trend in trapping layer intensity is observed, with generally weakest intensities in the early morning and strongest near sunset.

During the VOCAR experiment, average trapping layer base and top heights corresponding to SOCM 0, 12 and 24 hr over water forecasts were generally highest at offshore sites. At NTD, the model forecast many deep surface ducts and few significant elevated ducts, resulting in very low average trapping layer heights. On average, SOCM daytime (VT 00Z) forecasts of trapping layer height were quite similar at all forecast lengths; at night (VT 12Z), average model base and top heights increased about 200 m over the 12 to 24 hr forecast interval. At tau = 24 hr, the diurnal pattern in SOCM average trapping layer heights is in agreement with observed variability (i.e., lower in the afternoon, higher at night); on the contrary, at the 0 and 12 hr forecast lengths, model forecast trapping layer heights actually average less at night (VT 12Z) than during the day (VT 00Z). On average, forecast M-deficits are somewhat greater for 12 hr forecasts (as opposed to 24 hr forecasts) and during the daytime (i.e., at 00Z). Spatially, at tau = 24 hr, average forecast M-deficits were weakest at VOCAR southern coastal sites and strongest at the two island sites.

Comparisons made between SOCM analysis (tau = 0 hr) and background (12 hr model forecast verified at the analysis time) profiles indicated a rather limited impact of data assimilation during model initialization on refractive structure. Statistics indicate that, in the vast majority of cases (~ 88 %), SOCM first guess and analysis dominant trapping layers had identical base and top heights; on the contrary, only about 2 % of all analyzed cases had distinct background and analysis trapping layers. Analysis minus background absolute mean deviations

for trapping layer M-deficit were quite small, about one (two) M-units for SOCM over land (water) forecasts. In general, modifications in refractivity during model initialization were limited by poor vertical resolution of the analysis, and the critical omission of moisture as an analyzed variable.

SOCM 12 to 24 hr surface ducting performance statistics indicate a fairly decent capability (PF values ~ 1/3 to 1/2), but a rather limited reliability (PA ~ 0.2), in the forecasting of surface ducting. At all forecast lengths, no significant differences in either PF or PA scores are noted between SOCM water and land point forecasts, although the number of SOCM surface duct forecasts is considerably higher over water than land. On the other hand, PC and FAR scores corresponding to SOCM land point forecasts are better than comparable scores derived for SOCM over water forecasts. For both 12 and 24 hr forecasts, the PF and PA scores of both SOCM predictors are higher during the day (VT 00Z) than at night (VT 12Z); for the PC and FAR scores, the opposite occurs. In line with a much higher average trapping layer, the number of nighttime surface ducts forecast at tau = 24 hr is significantly less than at tau = 12 hr.

With regards to elevated trapping layer forecasting, the very high incidence of both observed and forecast trapping layers results in postagreement scores of 1, or nearly 1, for both SOCM predictors. At all forecast lengths, PF and PC scores corresponding to SOCM over water forecasts were considerably higher (in most cases, by about 0.2) than comparable scores for SOCM land point forecasts. For both 12 and 24 hr forecasts, all statistical indices for both SOCM predictors are higher during the day (VT 00Z) than at night (VT 12Z); however, day-night differences are generally not large. Finally, a comparison of SOCM 12 and 24 hr elevated trapping layer statistics indicates little difference in forecasting performance at these two forecast lengths.

For verification of trapping layer height and intensity, average error statistics (bias, MAE and RMSE) were computed for SOCM water and land point forecasts. At all forecast lengths, significant negative biases (indicating underforecasting) in trapping layer base and top heights were found for both SOCM predictors. Model MAE and RMSE statistics for trapping layer height were large, generally a few hundred meters. On average, SOCM also underforecast the intensity of the trapping layer, with negative biases more pronounced with SOCM land point forecasts (as opposed to SOCM over water forecasts). SOCM trapping layer M-deficit MAE and RMSE statistics are large, averaging almost 15 and 20 M-units, respectively, over the 12 to 24 hr forecast interval. At all forecast lengths, MAE and RMSE statistics for trapping layer intensity

are comparable for both SOCM predictors. Trapping layer intensity biases corresponding to the SOCM over water predictor are significantly less in magnitude than SOCM land point predictor biases. Based on day (VT 00Z) and night (VT 12Z) error statistics, SOCM's overall performance in forecasting trapping layer height and intensity is better during the daytime; for most statistics, day-night differences are less pronounced at tau = 24 hr (as opposed to tau = 12 hr). Finally, comparisons of SOCM error statistics at the 12 and 24 hr forecast lengths indicates overall better model performance in forecasting trapping layer height and intensity at the longer (24 hr) forecast length.

In order to investigate synoptic (large-scale) variability in observed and forecast VOCAR data, low-pass filtered composite time series of average trapping layer height and intensity were computed for both MRS observations and SOCM 12 and 24 hr water point forecasts. All average error statistics derived from forecast minus observed differences in 12 hr synoptic trend indicate better forecast performance for 12 hr persistence than for SOCM 12 or 24 hr forecasts. On average, SOCM 12 hr forecasts were somewhat better than those at 24 hr in predicting synoptic trends in trapping layer height. During VOCAR, SOCM's skill in predicting synoptic trends may have been negatively impacted by inaccurate time-dependent boundary conditions (from the operational global model) and inadequate updating of model conditions during incremental update (analysis) initialization.

Overall statistical results from this study indicate that the Navy's second order closure version of NORAPS performed well in short-range refractivity forecasting during the VOCAR experiment. However, results indicate that improvements are needed in model physics to rectify the problem of rather large negative biases in trapping layer height. Further, improvements are needed in the data analysis component of the forecast system, including higher vertical resolution (comparable to that of the forecast model) and inclusion of moisture as an analyzed variable. Given SOCM's high sensitivity to terrain type, select alterations in model topography (such as masking offshore islands) might prove beneficial to forecasting performance. As improvements continue to be implemented with SOCM, further evaluations should be carried out utilizing the VOCAR database. Additionally, SOCM's ability to forecast refractive structure needs to be tested under other types of environmental conditions, in other geographical regions and times of year.

ACKNOWLEDGMENTS

The author gratefully acknowledges the contributions of all personnel at NRL Monterey, Naval Postgraduate School in Monterey, and Naval Air Warfare Center Weapons Division at Point Mugu who were involved in the creation of the VOCAR observational and model database. Special thanks are extended to Mr. John Cook of NRL Monterey for his invaluable technical assistance. The support of the sponsor, the Office of Naval Research, under program element 0602435N, is gratefully acknowledged.

REFERENCES

Burk, S.D., and W.T. Thompson, 1989: A vertically nested regional numerical weather prediction model with second-order closure physics. Mon. Wea. Rev., 117, 2305-2324.

Goerss, J.S., and P.A. Phoebus, 1993: The multivariate optimum interpolation analysis of meteorological data at the Fleet Numerical Oceanography Center. Naval Research Laboratory, Monterey, CA, NRL/FR/7531--92-9413, 60 pp.

APPENDIX A - MRS Trapping Layers - Station Data

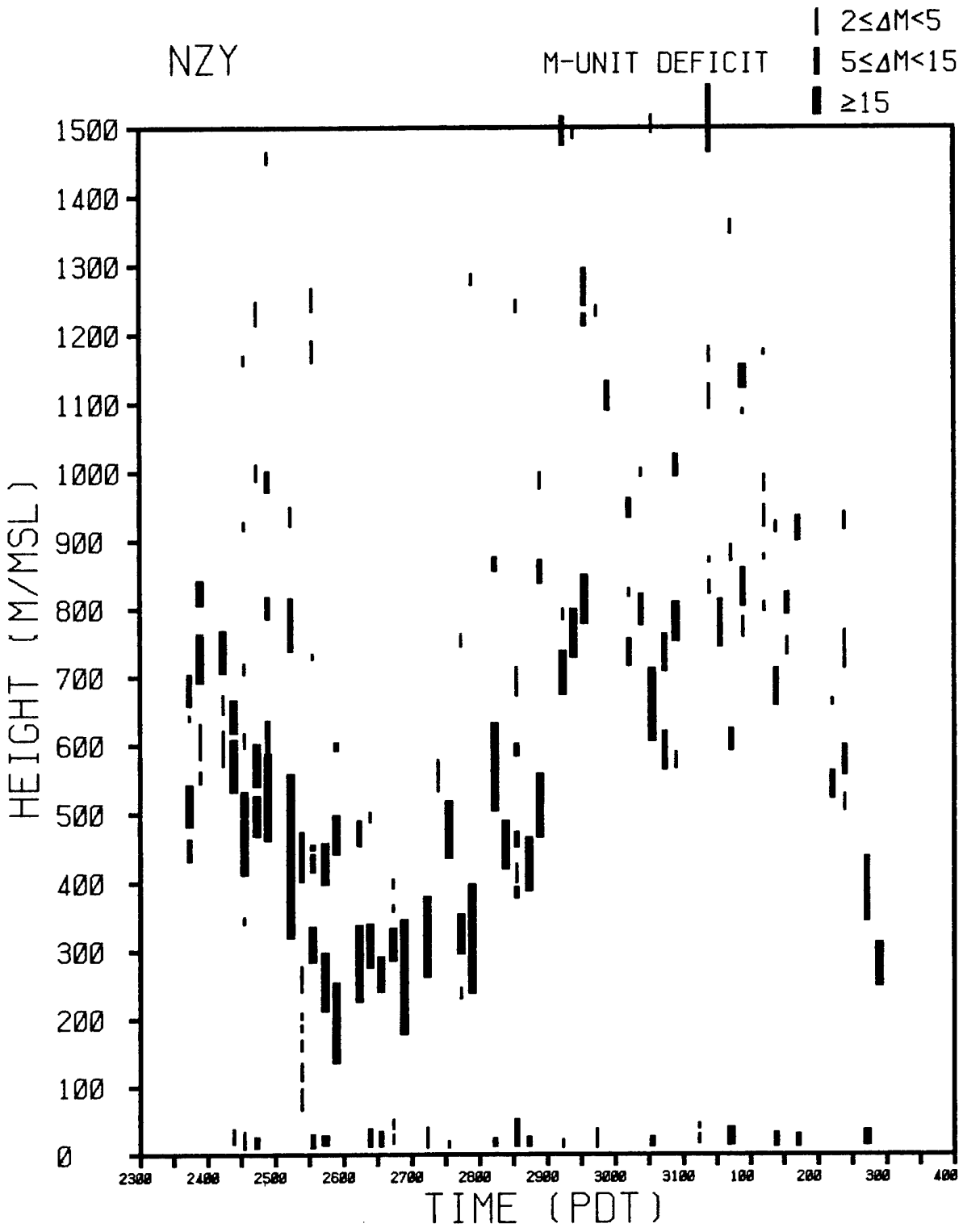
NZY
M-UNIT DEFICIT
2≤ΔM<5
5≤ΔM<15
≥15
HEIGHT (M/MSL)
1500
1400
1300
1200
1100
1000
900
800
700
600
500
400
300
200
100
0
2300
2400
2500
2600
2700
2800
2900
3000
3100
100
200
300
400
TIME (PDT)

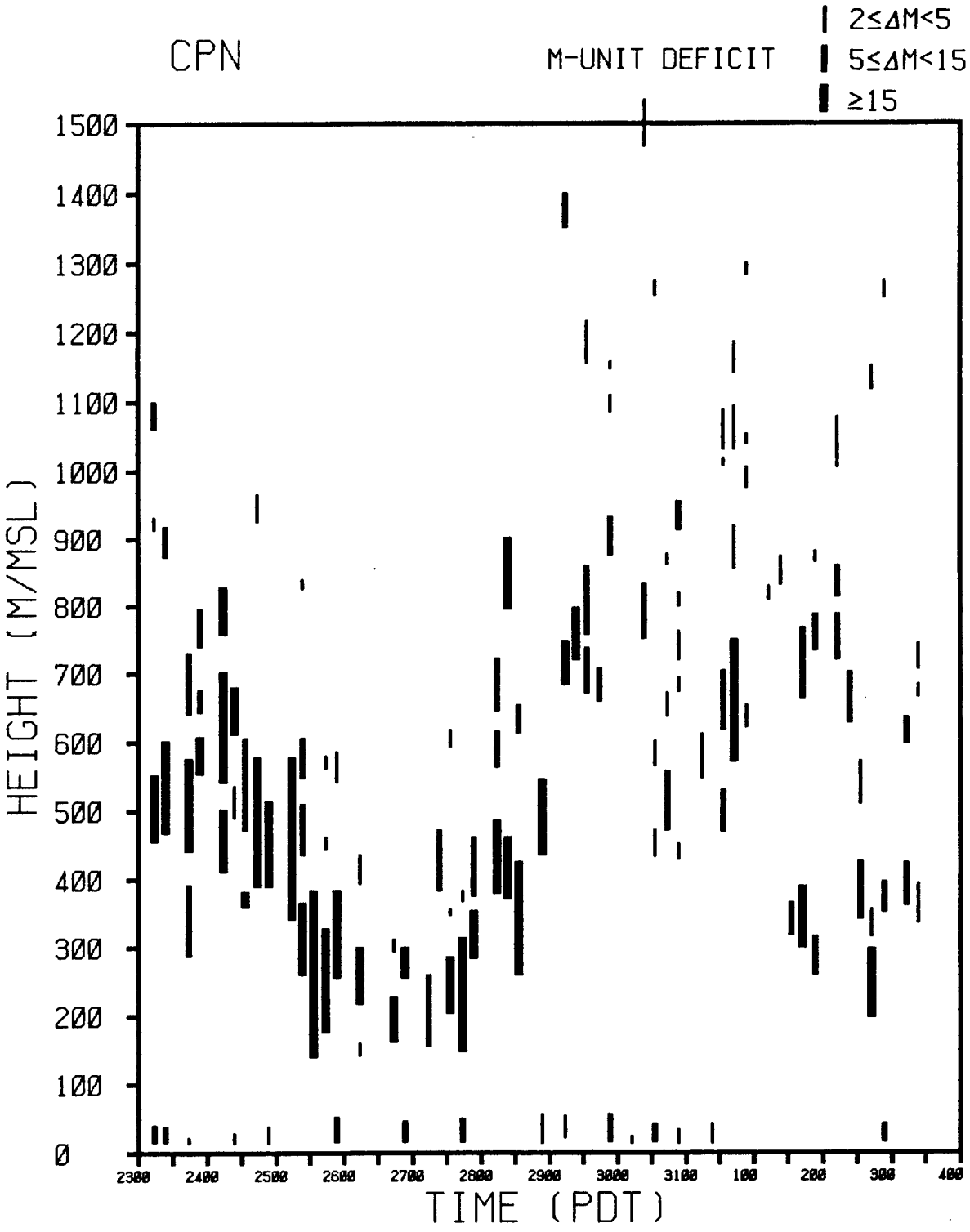
CPN
M-UNIT DEFICIT
2≤ΔM<5
5≤ΔM<15
≥15
HEIGHT (M/MSL)
1500
1400
1300
1200
1100
1000
900
800
700
600
500
400
300
200
100
0
2300
2400
2500
2600
2700
2800
2900
3000
3100
100
200
300
400
TIME (PDT)

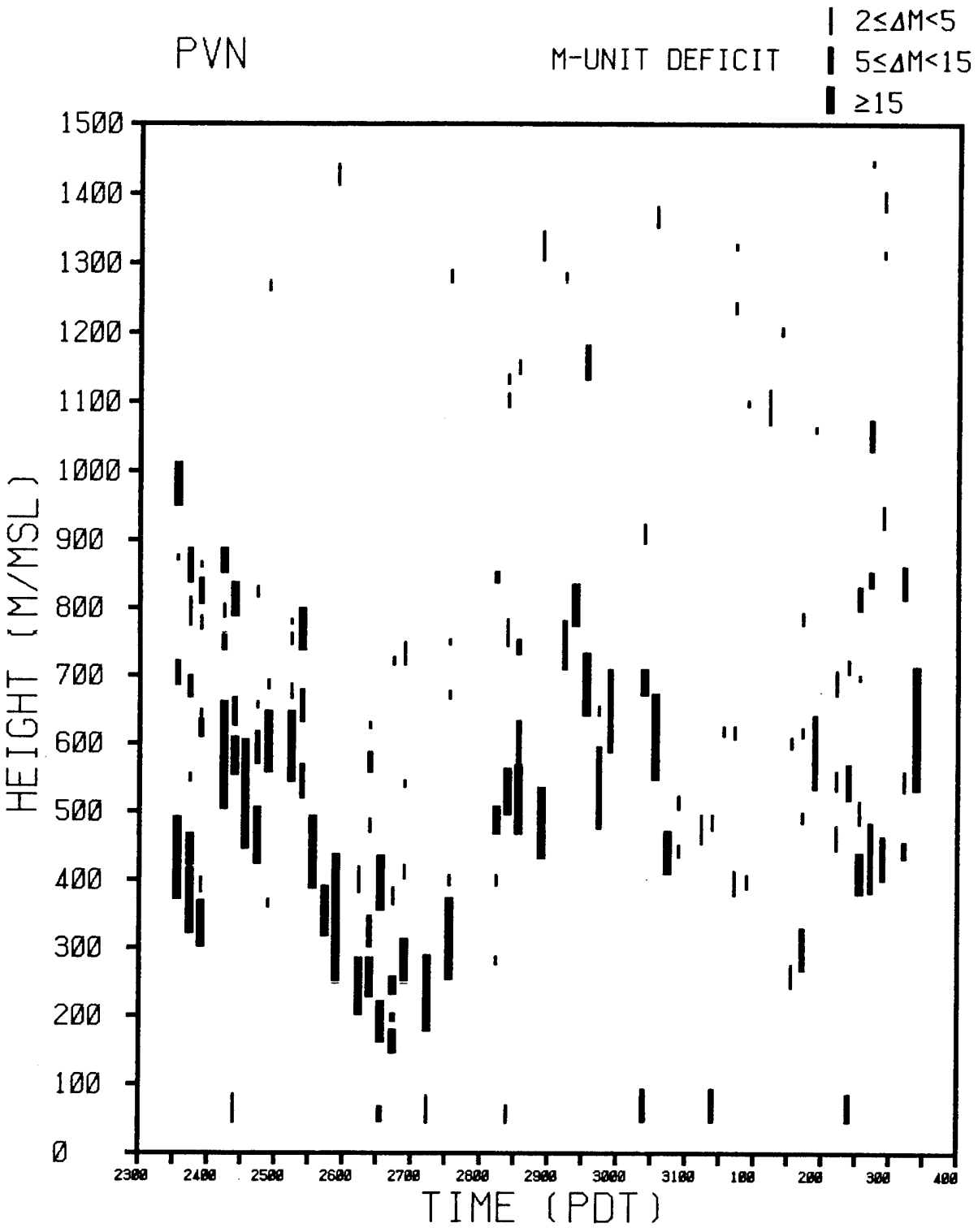
PVN
M-UNIT DEFICIT
2≤ΔM<5
5≤ΔM<15
≥15
HEIGHT (M/MSL)
1500
1400
1300
1200
1100
1000
900
800
700
600
500
400
300
200
100
0
2300
2400
2500
2600
2700
2800
2900
3000
3100
100
200
300
400
TIME (PDT)

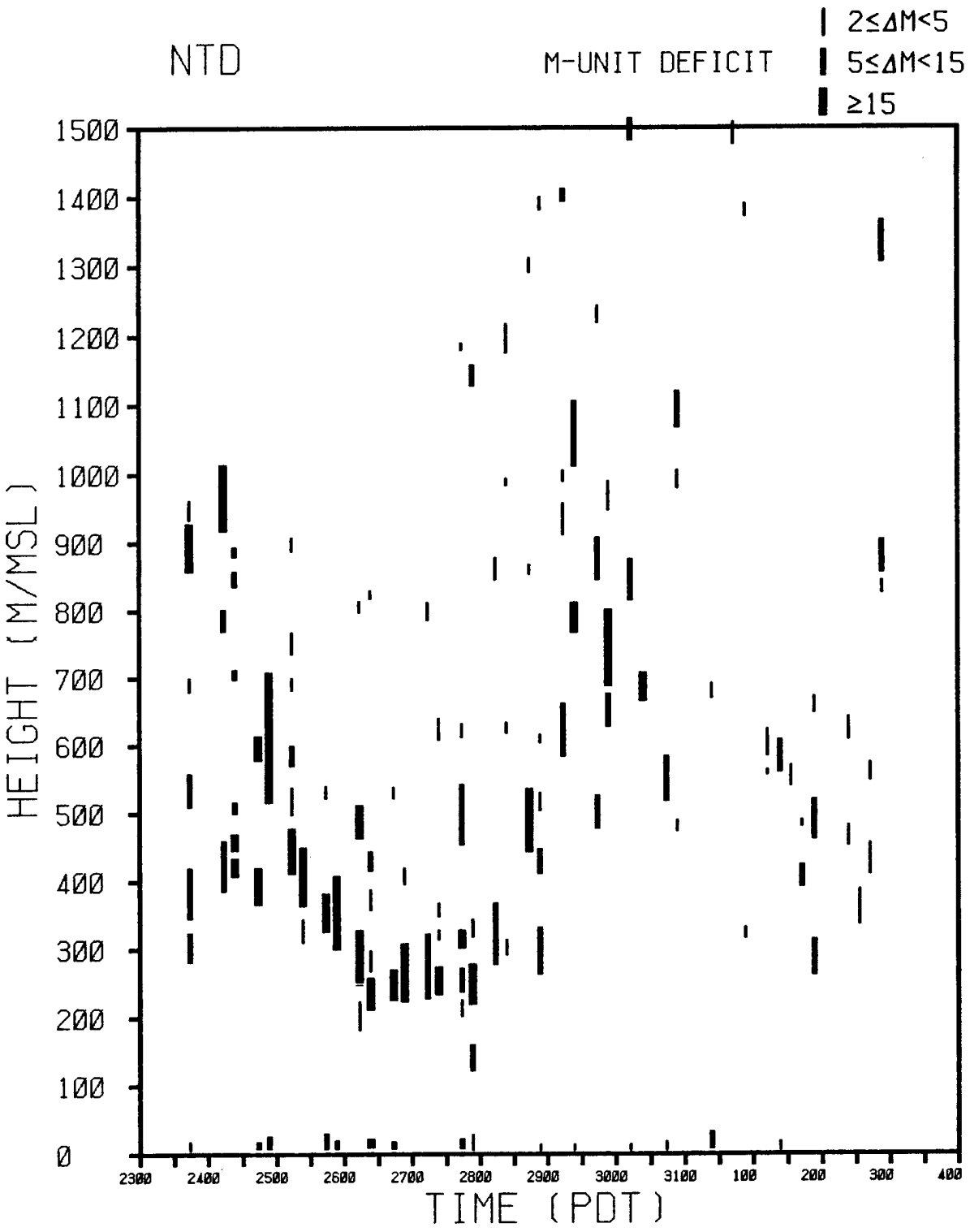
NTD
M-UNIT DEFICIT
2≤ΔM<5
5≤ΔM<15
≥15
HEIGHT (M/MSL)
1500
1400
1300
1200
1100
1000
900
800
700
600
500
400
300
200
100
0
2300
2400
2500
2600
2700
2800
2900
3000
3100
100
200
300
400
TIME (PDT)

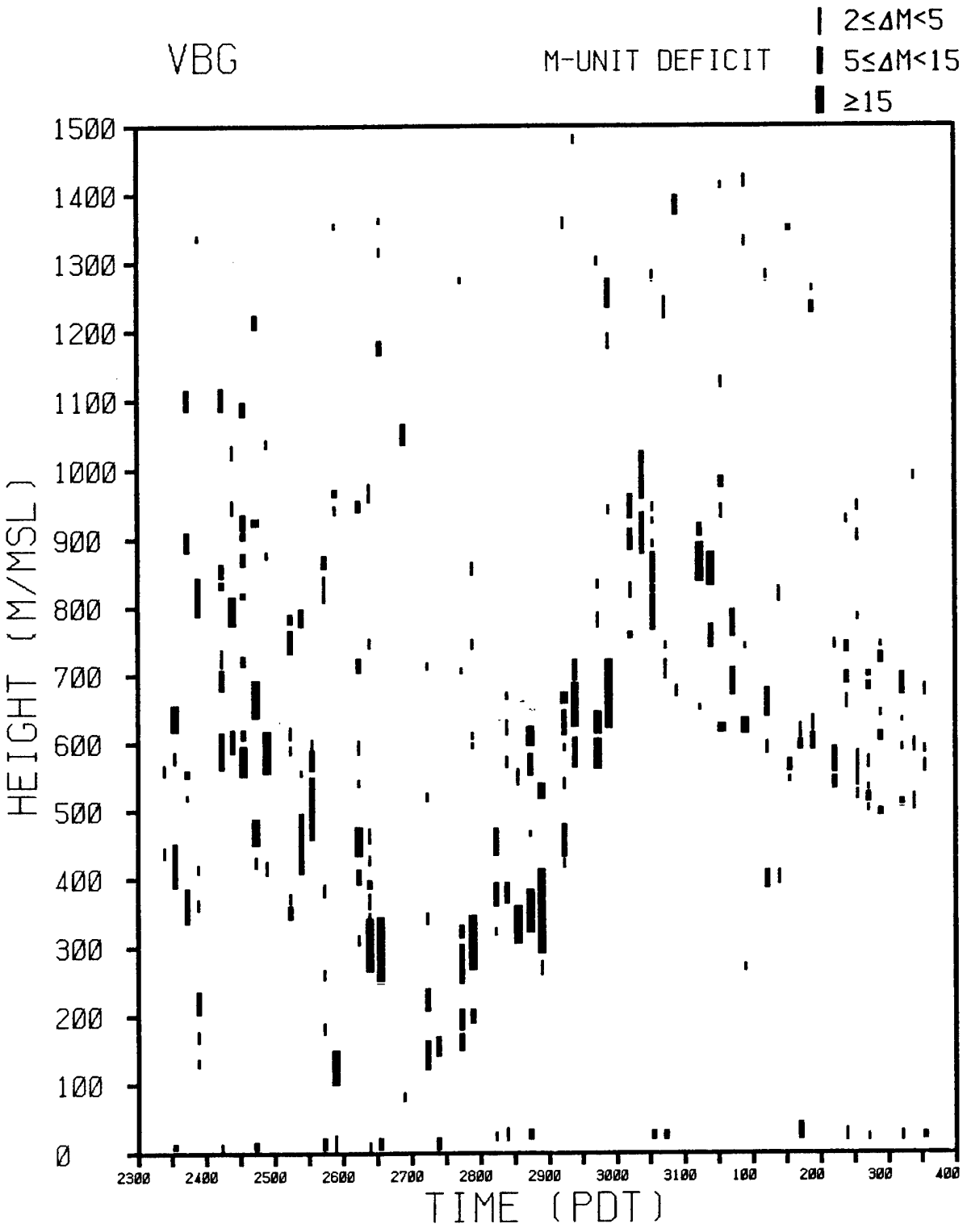
VBG
M-UNIT DEFICIT
2≤ΔM<5
5≤ΔM<15
≥15
HEIGHT (M/MSL)
1500
1400
1300
1200
1100
1000
900
800
700
600
500
400
300
200
100
0
2300
2400
2500
2600
2700
2800
2900
3000
3100
100
200
300
400
TIME (PDT)

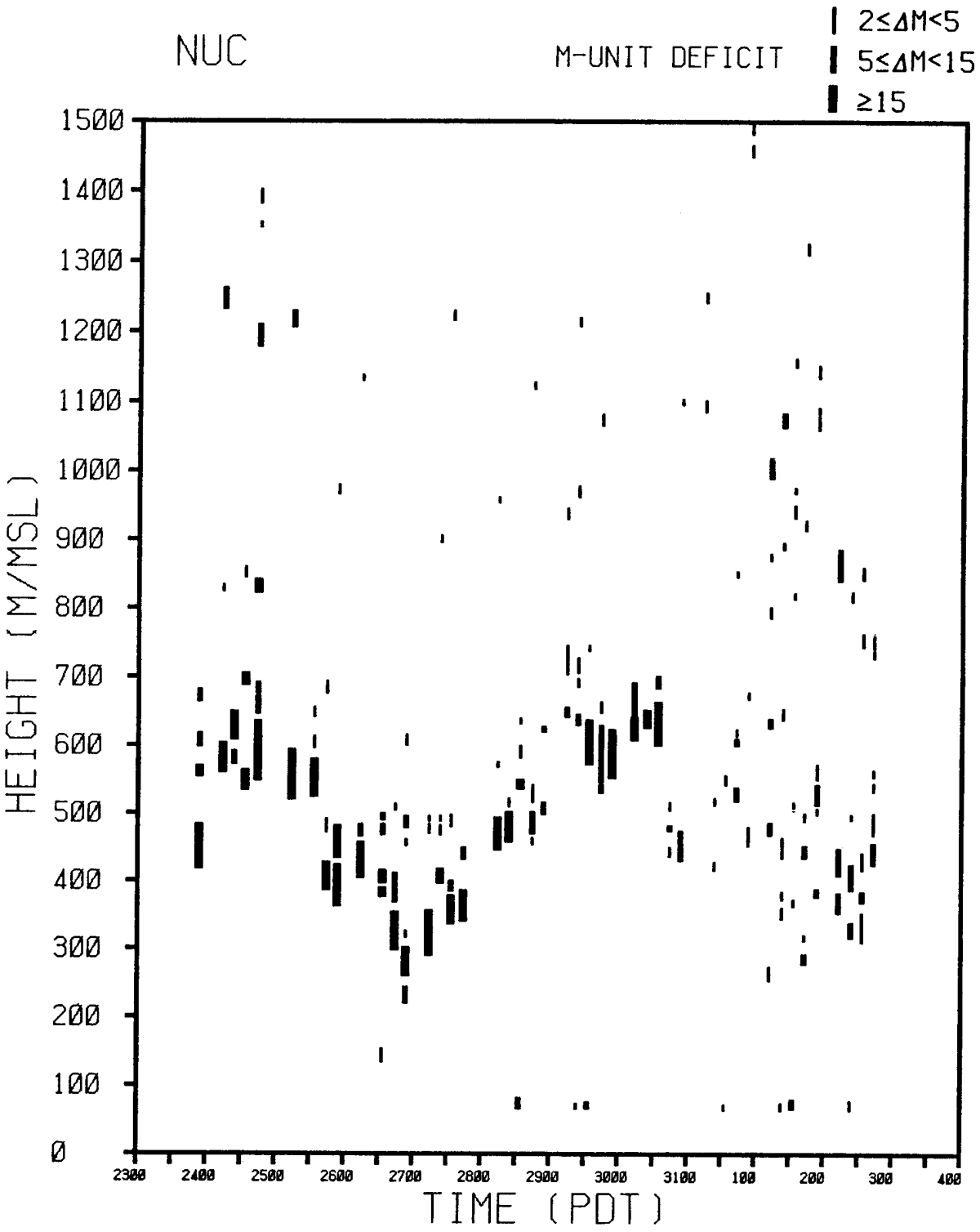
NUC
M-UNIT DEFICIT
2≤ΔM<5
5≤ΔM<15
≥15
HEIGHT (M/MSL)
1500
1400
1300
1200
1100
1000
900
800
700
600
500
400
300
200
100
0
2300
2400
2500
2600
2700
2800
2900
3000
3100
100
200
300
400
TIME (PDT)

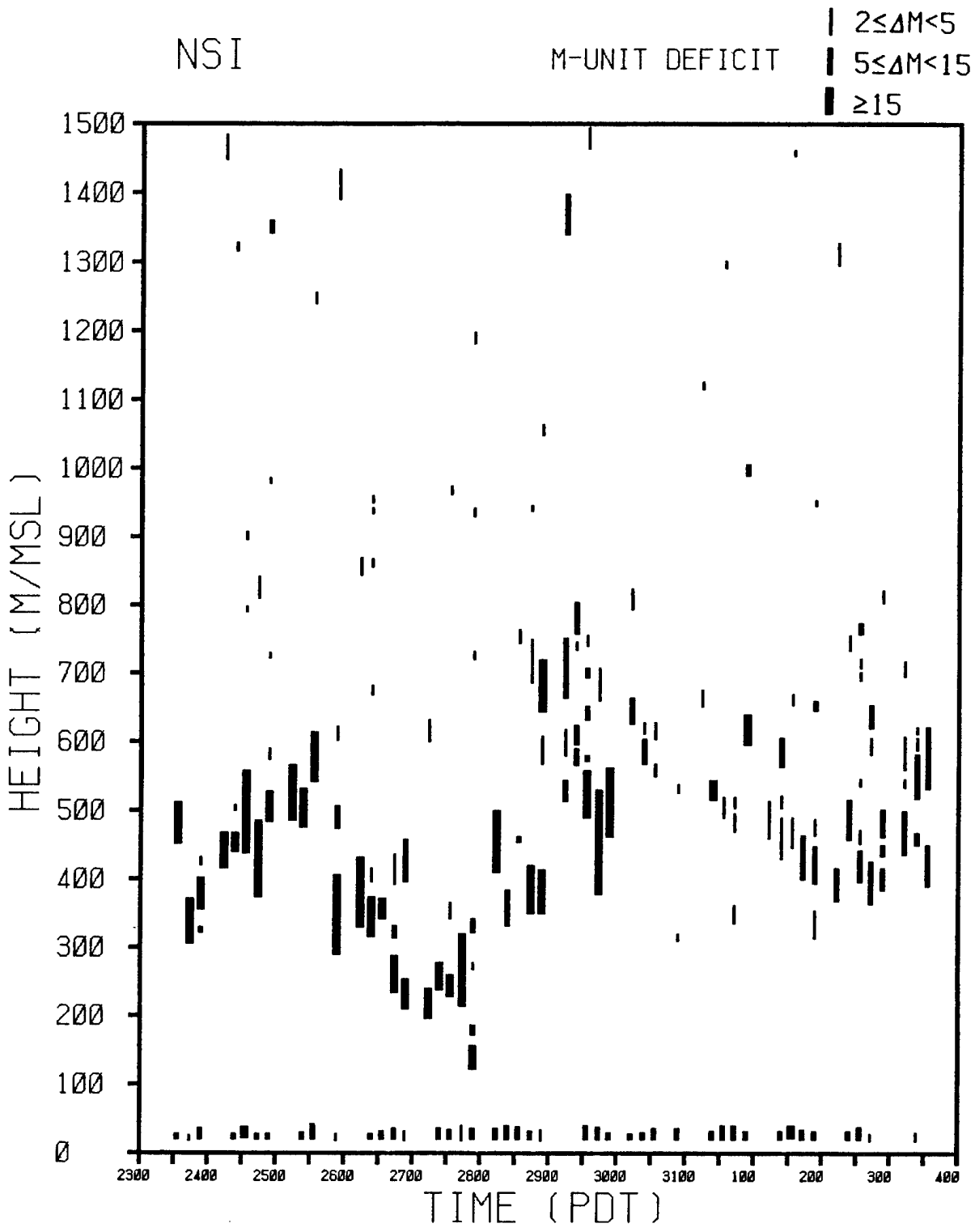
NSI
M-UNIT DEFICIT
2≤ΔM<5
5≤ΔM<15
≥15
HEIGHT (M/MSL)
1500
1400
1300
1200
1100
1000
900
800
700
600
500
400
300
200
100
0
2300
2400
2500
2600
2700
2800
2900
3000
3100
100
200
300
400
TIME (PDT)

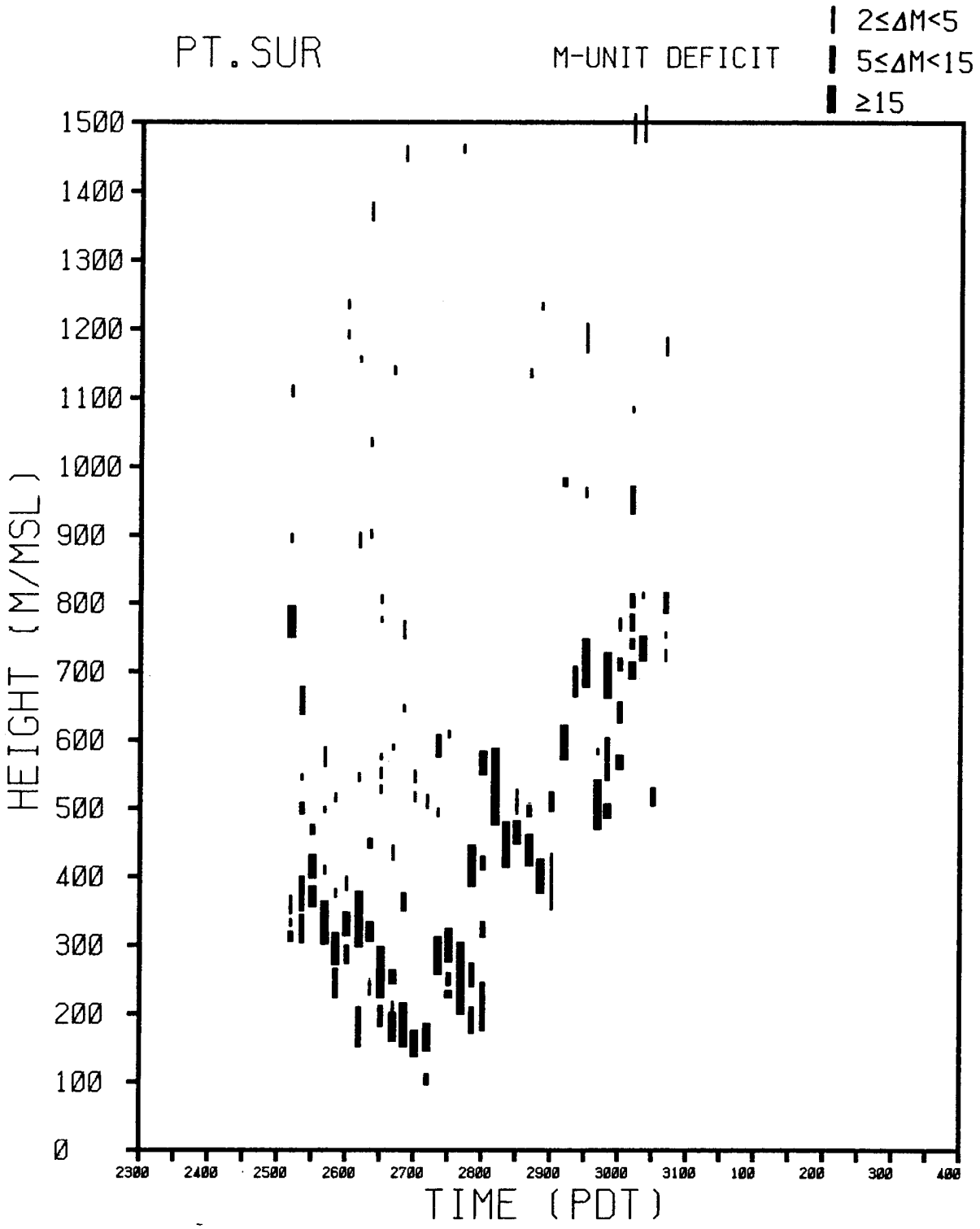
PT. SUR
M-UNIT DEFICIT
2≤ΔM<5
5≤ΔM<15
≥15
HEIGHT (M/MSL)
1500
1400
1300
1200
1100
1000
900
800
700
600
500
400
300
200
100
0
2300
2400
2500
2600
2700
2800
2900
3000
3100
100
200
300
400
TIME (PDT)

APPENDIX B - SOCM Trapping Layers - 12 and 24 hr Water Point Forecasts

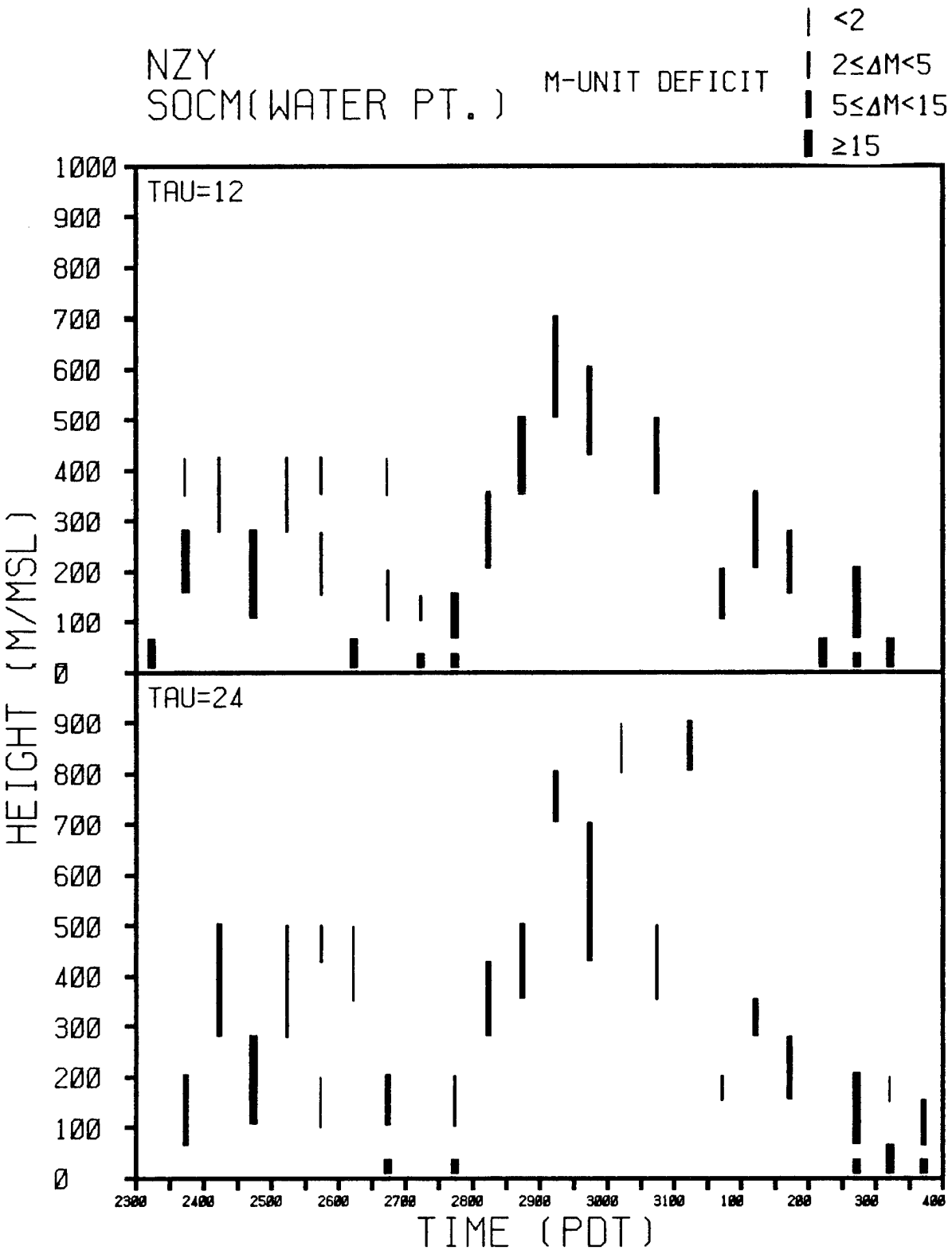
NZY
SOCM(WATER PT.)
M-UNIT DEFICIT
<2
2≤ΔM<5
5≤ΔM<15
≥15
TAU=12
TAU=24
HEIGHT (M/MSL)
1000
900
800
700
600
500
400
300
200
100
0
2300
2400
2500
2600
2700
2800
2900
3000
3100
100
200
300
400
TIME (PDT)

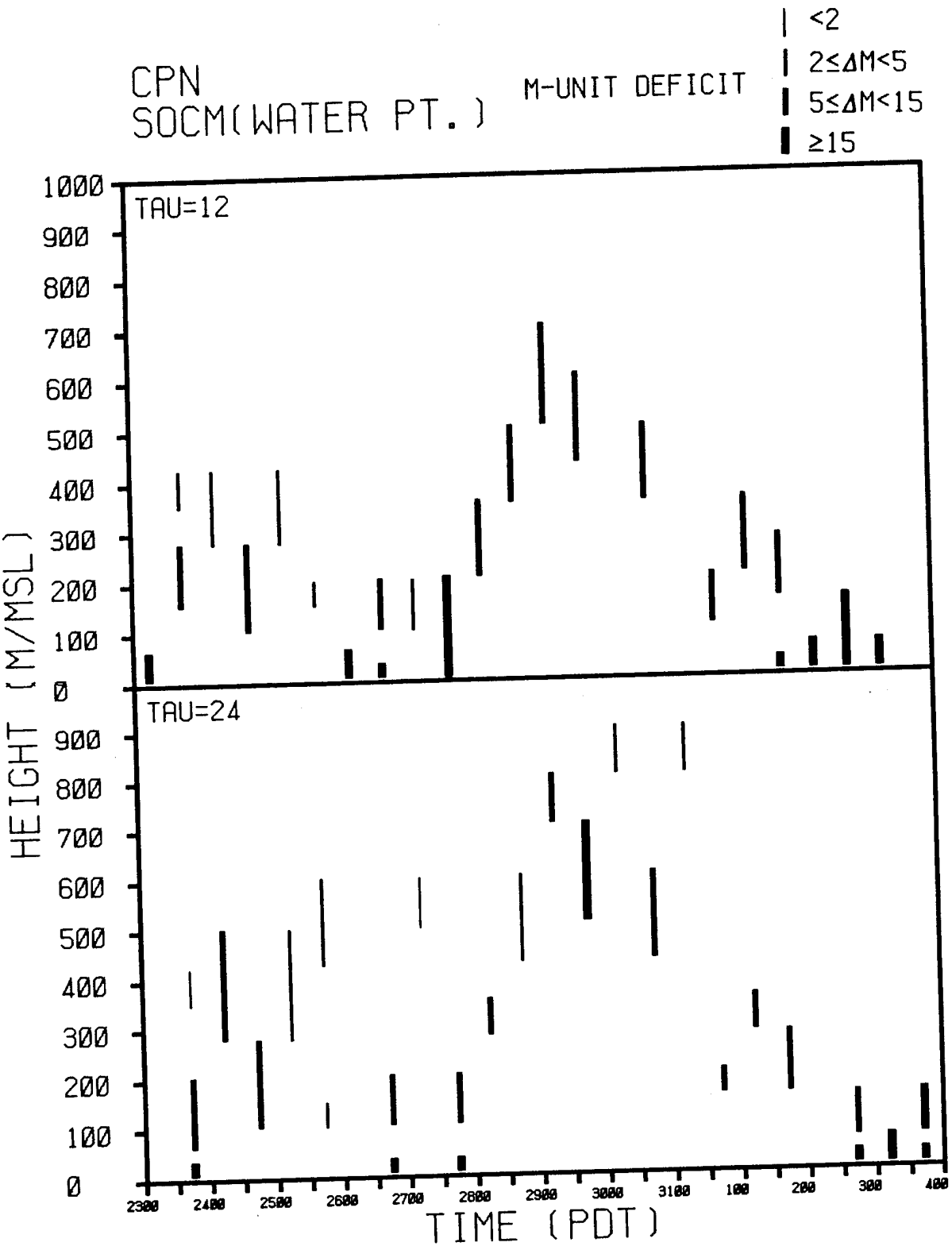
CPN
SOCM(WATER PT.)
M-UNIT DEFICIT
<2
2≤ΔM<5
5≤ΔM<15
≥15
TAU=12
TAU=24
HEIGHT (M/MSL)
1000
900
800
700
600
500
400
300
200
100
0
2300
2400
2500
2600
2700
2800
2900
3000
3100
100
200
300
400
TIME (PDT)

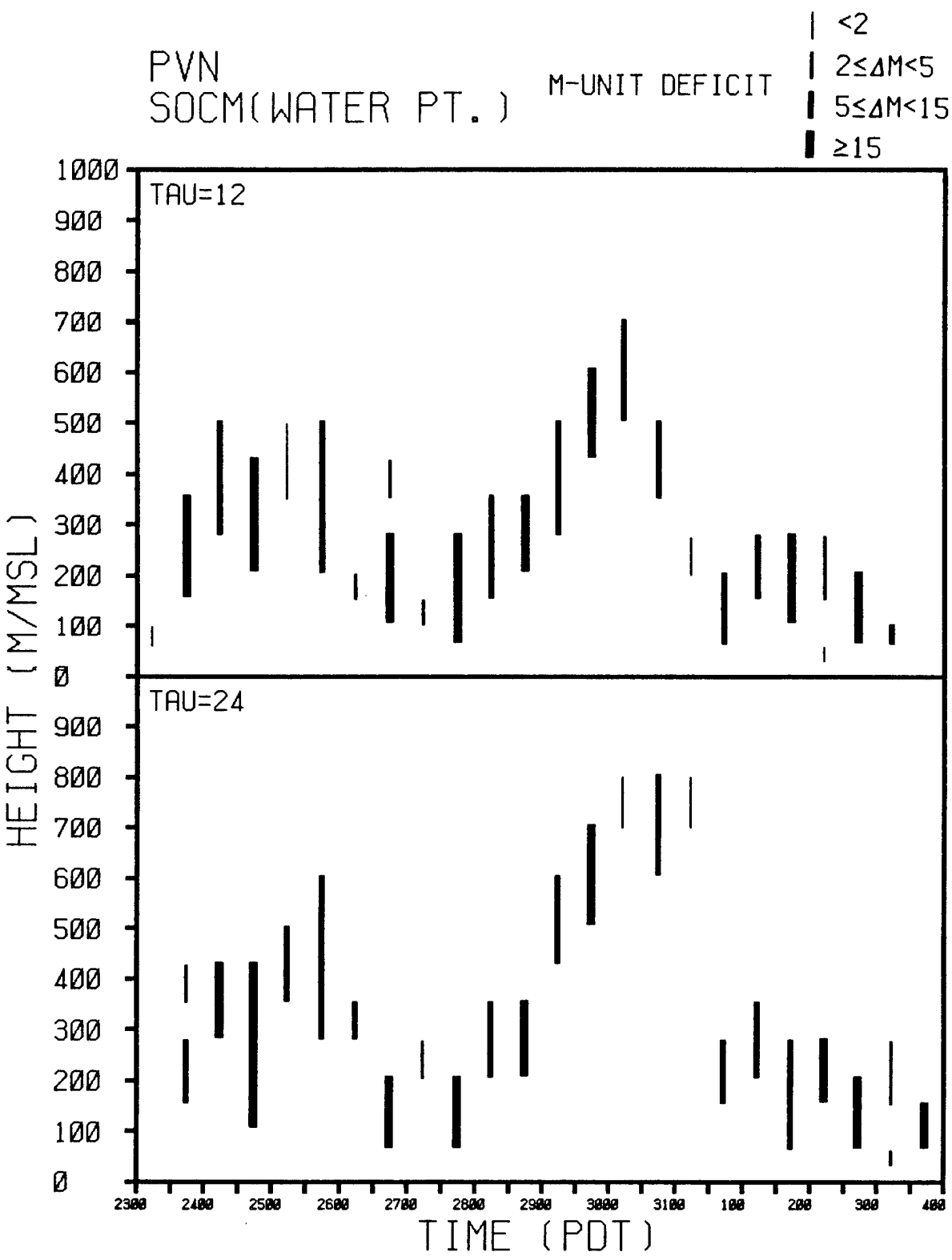
PVN
SOCM(WATER PT.)
M-UNIT DEFICIT
<2
2≤ΔM<5
5≤ΔM<15
≥15
TAU=12
TAU=24
HEIGHT (M/MSL)
1000
900
800
700
600
500
400
300
200
100
0
2300
2400
2500
2600
2700
2800
2900
3000
3100
100
200
300
400
TIME (PDT)

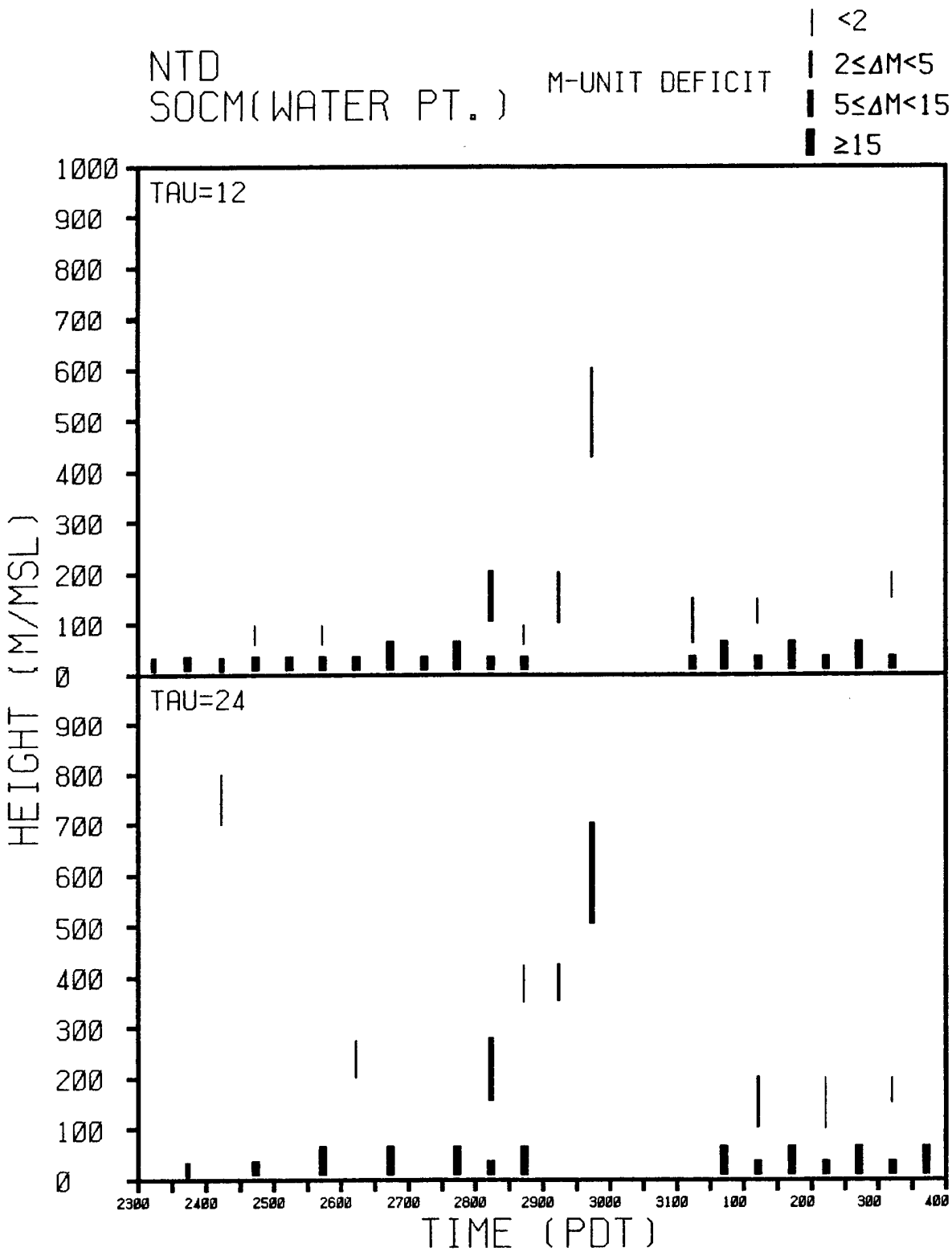
NTD
SOCM(WATER PT.)
M-UNIT DEFICIT
<2
2≤ΔM<5
5≤ΔM<15
≥15
TAU=12
TAU=24
HEIGHT (M/MSL)
1000
900
800
700
600
500
400
300
200
100
0
2300
2400
2500
2600
2700
2800
2900
3000
3100
100
200
300
400
TIME (PDT)

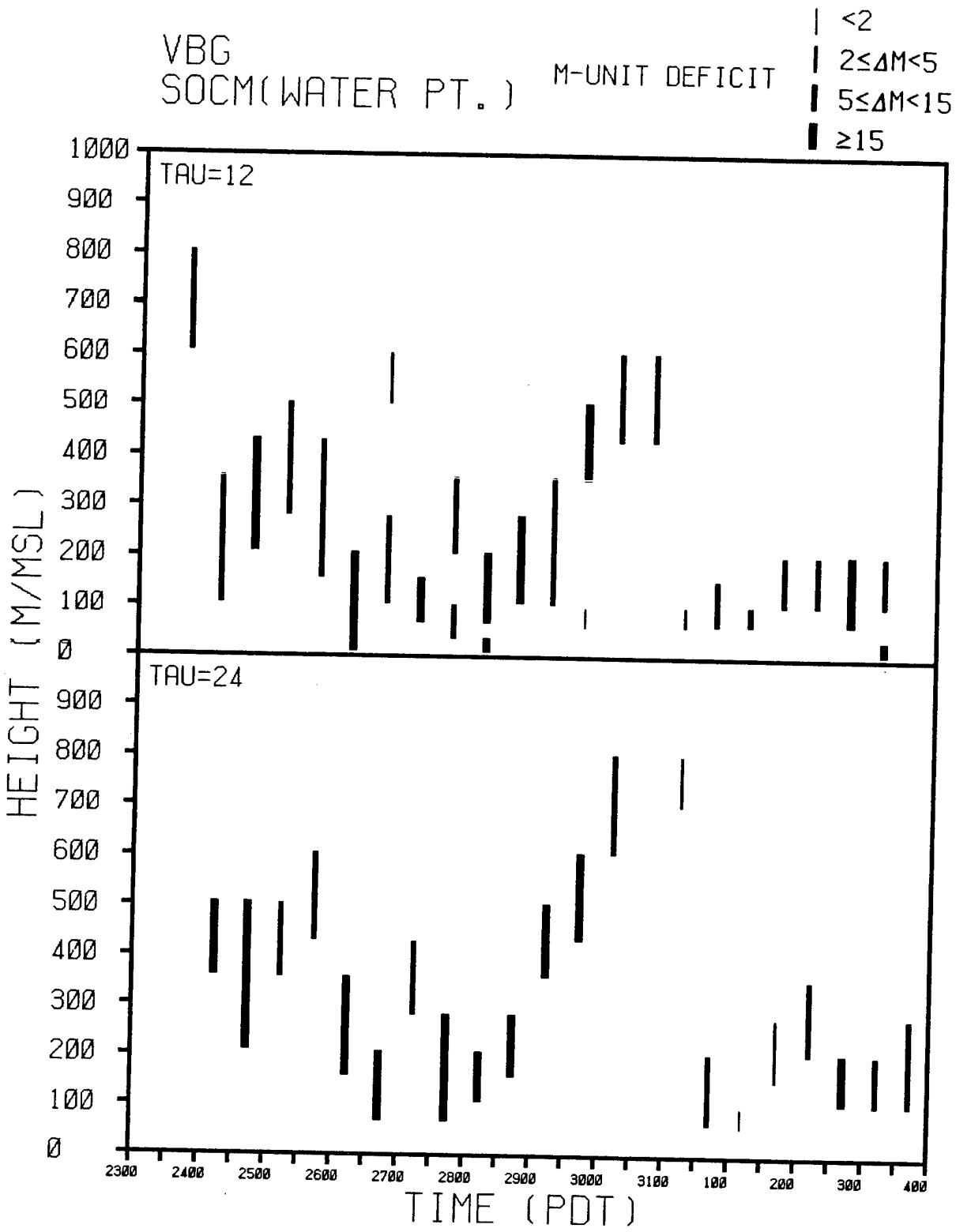
VBG
SOCM(WATER PT.)
M-UNIT DEFICIT
| <2
| 2≤ΔM<5
| 5≤ΔM<15
| ≥15
TAU=12
TAU=24
HEIGHT (M/MSL)
1000
900
800
700
600
500
400
300
200
100
0
2300
2400
2500
2600
2700
2800
2900
3000
3100
100
200
300
400
TIME (PDT)

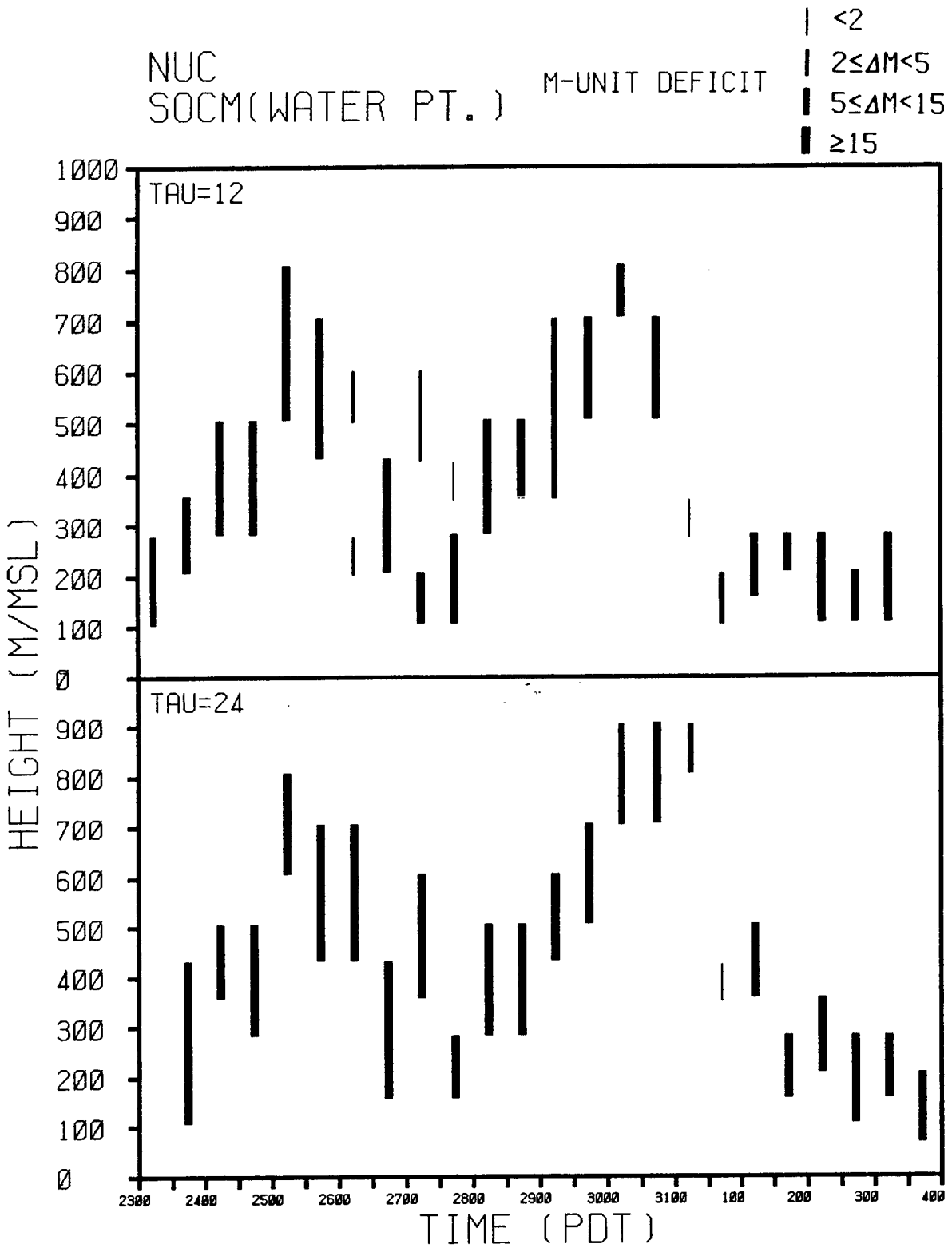
NUC
SOCM(WATER PT.)
M-UNIT DEFICIT
<2
2≤ΔM<5
5≤ΔM<15
≥15
TAU=12
TAU=24
HEIGHT (M/MSL)
TIME (PDT)
0
100
200
300
400
500
600
700
800
900
1000
2300
2400
2500
2600
2700
2800
2900
3000
3100
100
200
300
400

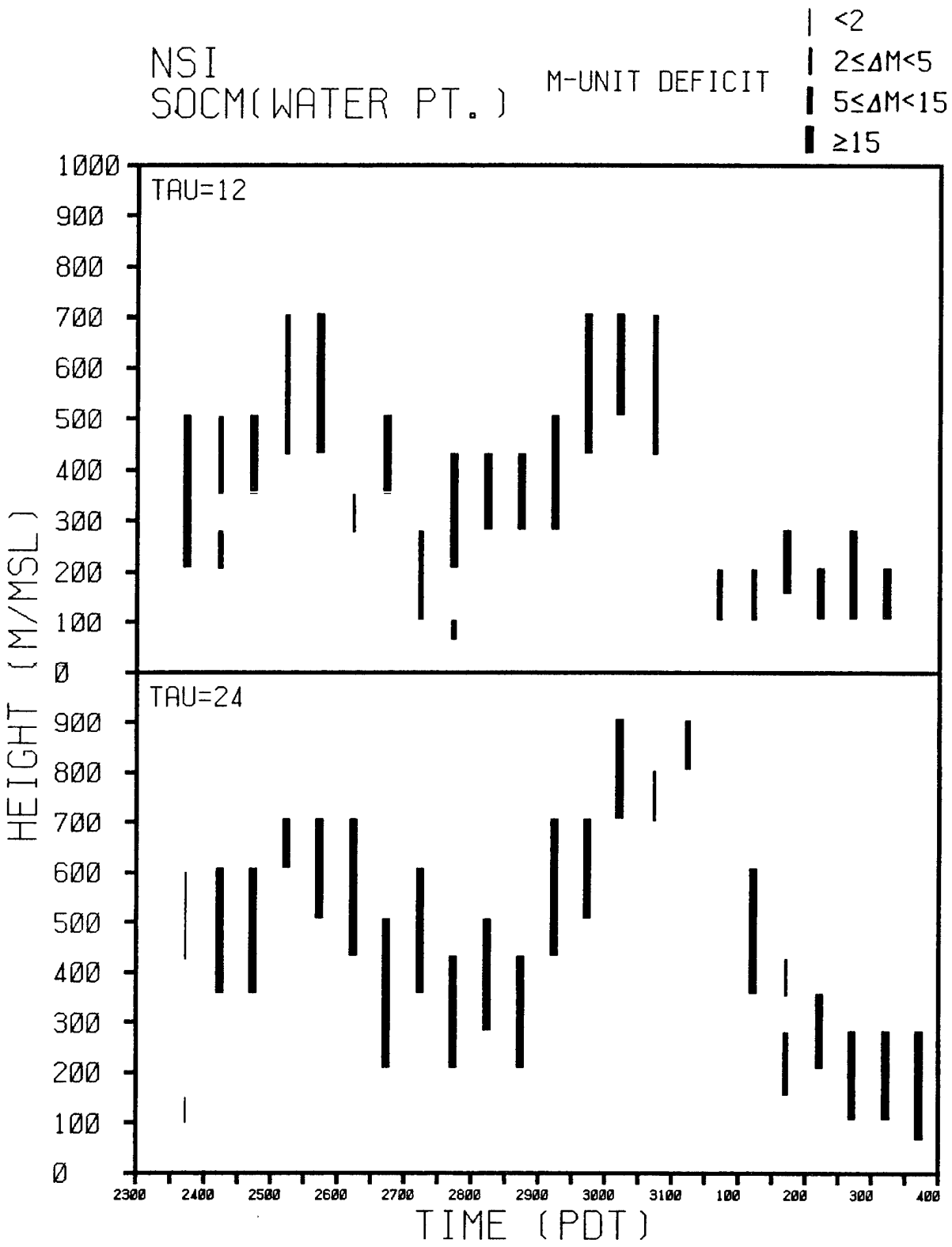
NSI
SOCM(WATER PT.)
M-UNIT DEFICIT
<2
2≤ΔM<5
5≤ΔM<15
≥15
TAU=12
TAU=24
HEIGHT (M/MSL)
1000
900
800
700
600
500
400
300
200
100
0
2300
2400
2500
2600
2700
2800
2900
3000
3100
100
200
300
400
TIME (PDT)

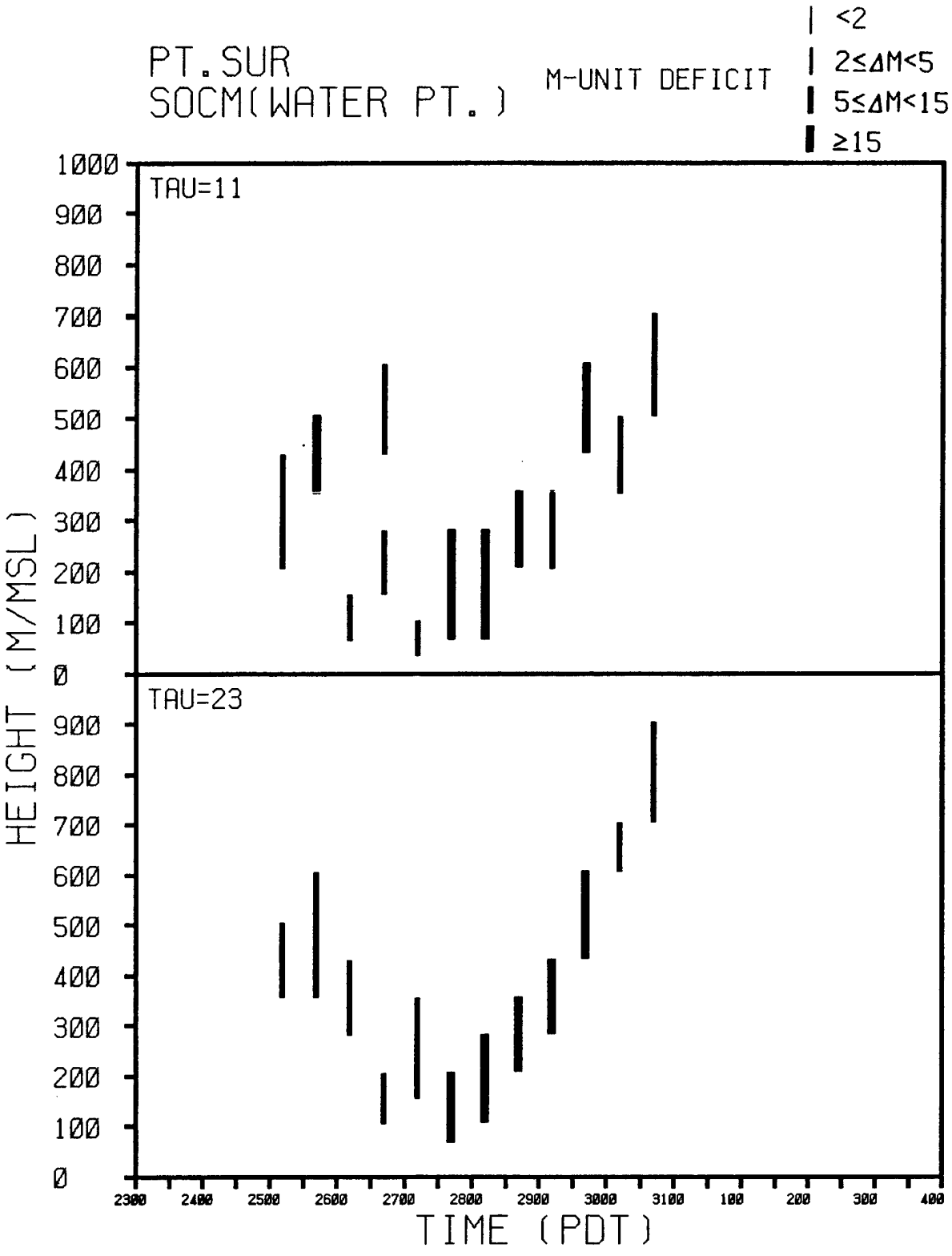
PT.SUR
SOCM(WATER PT.)
M-UNIT DEFICIT
<2
2≤ΔM<5
5≤ΔM<15
≥15
TAU=11
TAU=23
HEIGHT (M/MSL)
1000
900
800
700
600
500
400
300
200
100
0
2300
2400
2500
2600
2700
2800
2900
3000
3100
100
200
300
400
TIME (PDT)